PLEXIN-A4 RECEPTOR REGULATES DENDRITE MORPHOGENESIS IN RESPONSE TO CLASS 3 SEMAPHORIN 3A SIGNALING IN MOUSE PYRAMIDAL NEURONS

by

SHENG-SHIANG (ANSON) PENG

A Dissertation submitted to the

Graduate School-Newark

Rutgers, The State University of New Jersey

in partial fulfillment of the requirements

for the degree of

Master of Science

Graduate Program in Biological Science

written under the direction of

Dr. Tracy Tran

and approved by

_____

_____

_____

Newark, New Jersey

October, 2014

ABSTRACT OF THE DISSERTATION

Plexin-A4 receptor regulates dendrite morphogenesis in response to Class 3 Semaphorin 3A signaling in mouse pyramidal neurons

By Sheng-Shiang (Anson) Peng

Dissertation Director:

Dr. Tracy Tran

Abstract

The formation of a complex nervous system requires precise navigation and elaboration for growth cone and dendrites to connect to their target. During development, guidance molecules and receptors control the majority of the circuitry events, including promotion or inhibition of neurite growth. Semaphorin 3A, a secreted Class 3 Semaphorin member, is well known for its chemorepellent function on growth cone mediated by the Neuropilin1/PlexinA4 holoreceptor complex. Recently, it has been shown to have opposite cellular responses in promoting dendrite growth and branching in mouse cortical pyramidal neurons (*1*, *2*). However, the mechanism underlying how Semaphorin 3A/Neuropilin1/Plexin-A4 signaling regulates dendrite elaboration is unclear. Here, I have shown the importance and function of three distinct domains in the cytoplasmic region of the signaling transducing receptor of Semaphorin 3A, Plexin-A4, in regulating cortical neuron dendritic morphology. Both the C1 and H/RBD domains were found to be sufficient to trigger cortical pyramidal neuron dendrite elaboration, while the C2 domain was not necessary for dendrites growth and branching. Using biochemical and molecular methods in combination with *in vitro* assays, I found and

demonstrated that the Rho-GEF, FARP2 associates with PlexinA4 and mediates dendritic elaboration in primary cortical neurons following the ligand, Semaphorin 3A activation of the signaling pathway. In addition, I demonstrated that Plexin-A4 extracellular domains could interact with its co-receptor Neuropilin1, independent of the ligand Semaphorin 3A. Therefore, the extracellular Semaphorin domain may play a role in preventing Plexin-A4 activation, consistent with previous studies (*3, 4*).

Previously, another member of the Type A Plexin receptor, Plexin-A3, was shown to play a key role in inhibiting cortical neuron dendritic spine morphogenesis in vivo (*2*). However, the mechanism of how Plexin-A3 signals to restrain spine formation is unknown. I have generated an array of Plexin-A3 cytoplasmic deletion mutant constructs, analogous to the Plexin-A4 deletion mutants used for this study for future studies in investigating cortical neuron dendritic spine morphology. These molecular tools that I have developed will be useful for researchers to investigate the intracellular signaling mechanisms of Semaphorin signaling in regulating neuron morphology. Taken together, my findings provide new insights to Plexin-A4 signaling, in particular, highlighting distinct intracellular domains and downstream effectors required for promoting dendritic morphology.

Keywords: Plexin, Semaphorin, Pyramidal neuron, Dendrite, Morphology

Table of Contents

List of Figures

List of Tables

Acknowledgements

With so many to acknowledge, I would like to express my sincerest gratitude to all of the many people who provided me with the support without which the completion of this thesis would not have been possible. First, I must sincerely acknowledge my supervisor, Dr. Tracy Tran, who brought me into the most exciting research field and offered me a great project. I would also like to thank her for her patient supervision and extensive support in this project and in my daily life. During the time in the lab, I learned not only the knowledge of neuroscience but also the logic and critical thinking necessary to be a good scientist. I would also like to express my gratitude to the following people for their support and assistance in my study.

My committee members, Dr. Patrice Maurel and Dr. Gal Haspel. Thank you for being so involved as my committee.

I would like to extend a special thank you to our collaborator, Dr. Avraham Yaron, who provided the Plexin constructs and helped with publishing the paper. I also say thank you to Dr. Guy Mlechkovich and all of the Yaron Lab's members.

Thank you to all the members of the Tran Lab for your help throughout my time here: Dr. Berenice Hernandez-Enriquez, Dr. Ruihe Lin, Dr. James Reilly, Edward Martinez, Cathryn Rapadas, Richard Mariani, Beril Ozden, Matthew Gavin, and all the undergraduate students. Thank you all for your valuable help, discussions, suggestions, and technical support.

I would like thank Dr. Wilma Friedman for giving important feedback on my dendrite project. I want to also thank Dr. Nan Gao and Dr. Haesun Kim for letting me use their reagent and equipment. T

Thank you all the graduate students and postdocs who provided helpful discussions and opinions on the experiments and offered generous help.

I sincerely thank my wife, parents, and all my family members in Taiwan for their persistent and warm support. When I was almost exhausted by my experiments, they gave me consolation and motivation. Without their support, I would not have finished my degree successfully.

Thank you, everyone!

Chapter I Introduction

Beginning with the stunning work of Ramón y Cajal (5), the mammalian nervous system's wiring profile has been revealed. However, the mechanisms underlying how neuronal connections are formed and maintained remain largely unclear. Some fundamental questions include: 1) How do neurons determine the proper trajectory to extend their axons and dendrites? and 2) How do the external guidance molecules instruct neurons to form their proper connections? Furthermore, it has been shown previously that many guidance cues can control both axonal guidance events and the formation of dendritic morphology. The mechanistic logic underlying this multi-functionality is not known. In this study, I investigated how the same extracellular guidance cue signaling through the same receptor complex (same ligand-receptor pair) can repel peripheral nervous system (PNS) sensory axons by collapsing their growth cones and promote central nervous system (CNS) pyramidal neuron dendrite elaboration during development.

1.1 Nervous system and neuronal connection

The mammalian nervous system is highly connected bilaterally from rostral to caudal. The individual building block of the system is a single nerve cell called a neuron. Billions of neurons extend polarized axon and dendrites to connect and form the peripheral and central nervous systems. The Central Nervous System (CNS) includes the brain and spinal cord. One of its fundamental role is to process and integrate sensory information from the external environment and generate the appropriate behavioral response. The Peripheral Nervous System (PNS) is composed of the peripheral nerves,

including those emanating from sensory and motor neurons. These neurons are responsible for relay information to and from the brain.

Neurons are highly polarized cells with diverse morphology, and their unique morphology is tightly associated with their specific function (*6*). A typical neuron is divided to cell body (soma), dendrites and axon. Neurons extend dendrites/axons forming connections, synapses, in order to receiving or sending information from all over the body. It is extremely important for these dendrites to form correct branching, pattern, and density to establish the proper connection. If the connection is not properly formed, it could cause many different mental disorders or diseases. For instance, during the early development of children, aberrant dendritic arborization might contribute to their mental retardation or autism spectrum disorders (ASD) (*7*, *8*).

Previous research have shown the neural connection and wiring processes are largely regulated by external guidance molecules, which initiate inner cellular signaling cascades and change cell morphology and synapse formation (*9*, *10*). These molecules either function as chemorepellent to inhibit neurites or chemoattractant to promote/attract neurites. Many studies have shown that guidance molecules affect axon growth cone pathfindings and synapse formation (*11–17*). However, the mechanisms of how guidance cues regulate neuronal dendrites processes are relatively less well known. Thus, it would be interesting and important to investigate how guidance molecules affect dendrites outgrowth and synapse formation.

1.2 Pyramidal neurons and their dendritic development

Neurons are highly polarized with diverse morphology that make them unique from other cells. One of example is pyramidal neuron in the cerebral cortex. Pyramidal neurons are first discovered and studied by Ramón y Cajal and are abundant in the mammalian cerebral cortex, as well as in birds, fish, and reptiles (*18–20*). These neurons are mostly excitatory cells and mostly found in forebrain structures including the cerebral cortex, the hippocampus, and the amygdala. These structures are associated with higher cognitive functions, which indicate that pyramidal neurons are playing critical roles (*21*).

Layer V pyramidal neuron is one of the two well-studied pyramidal neurons (another is hippocampal neuron) because of its critical function (*21*). Like most neurons, layer V pyramidal neurons have multiple dendrites and a single axon (Figure 1). In addition, these neurons are characterized by the presence of separate basal and apical dendritic trees. During development, neurons extend a long but less branched apical dendrite at the apex of the cell body (soma) and relatively shorter but more branching basal dendrites at the opposite side. Layer V pyramidal neuron is also well known for its studded dendritic spines (*22*). Spines are small membranous protrusion structures on the dendrite. They receive input (mostly excitatory) from the axon (*21, 23*). A single dendrite can have hundreds thousands spines that significantly increase the possibilities of connecting to other neurons and more efficiently transduce the stimuli (*21*).

Years of studies have revealed that extracellular signals induce pyramidal neuron cell polarity and regulate dendrite and axon path finding as well as synapse formation (*9, 10*, *24*, *25*). Extracellular guidance cues induce intracellular signaling by changing the cytoskeleton network, such as actin assembly that leads to altered neuronal morphology and dendritic arborization (*26*). Therefore, studying the function of these guidance

molecules in the neuron development will benefit us in further understanding the development of the nervous system.

1.3 Guidance molecule family of Semaphorins and their receptors

Many guidance molecules and receptors complex have been discovered and are involved in axon/dendrite processes extension and synapse formation from embryonic to postnatal stage (*27–29*). Families of guidance cues such as Slits, Netrin, Ephrins, and Semaphorins are usually express in or around the target area or on the neuron itself, which either repel or attract the neuronal processes. Some of the guidance molecules such as Ephrins and class 4-7 Semaphorins are membrane bond proteins (*30*). These molecules function as short-range guidance cue. On the other hand, Slits, Netrins, and members of the class 3 Semaphorins are secreted proteins and these molecules may regulate from both short- and long-distance guidance.

Semaphorin is a large protein family involved in many pathways in neural development. Semaphorin was first discovered by Kolodkin and colleagues in 1992, who were studing the role of semaphorins in axon guidance (*31*). One year later, Luo et al. (1993) reported that Collapsin-1 (now type A class 3 Semaphorin, Sema3A) can cause growth cone repulsion in chicken brain (*32*). The Semaphrin family consists of eight subclasses and at least 27 members across different species from *C. elegans*, drosophila, zebrafish, rodents, to humans (*9*, *30*) (Figure 2). Many studies have shown that Semaphorins are involved in cardiovascular development, immune system function, cell migration, and even cancer(*33–35*). However, the class 3 secreted semaphorins have well-known functions in both the CNS and PNS during development; they are strong

repellents for various neuron growth cones, pruning factors for hippocampal neurons and negatively regulate excitatory synapse formation and distribution on cortical and hippocampal neurons, and most recently, they promote basal dendrite elaboration in cortical pyramidal neurons (*30*, *36–38*).

Class 3 Semaphorins are the most studied in the mammalian nervous system. They are secreted molecules and regulate neurons in short and long distances. As mentioned earlier, Semaphorins are strong inhibitory guidance molecules that will cause neuron axon growth cone collapse. Interestingly, recent studies have shown that the class 3 Semaphorin, Sema3A, signaling through the same receptor, Plexin-A1, can collapse axonal growth cones and promote neuron dendrite outgrowth and branching (*1*, *2*, *29*). How is the same molecule inducing two different cellular responses?

Plexins are phylogenetically conserved transmembrane protein families consisting of four subclasses and at least nine members across species in both vertebrate and invertebrate (*30*, *39*). Studies showed that Plexins contain a conserved Sema domain and divergent extracellular domains. Intracelluarlly, the Plexin cyto-domains contain two distinct segments: the C1 and C2domains, which are phylogenetically similar to a Ras guanosine triphosphatase (GTPase) activating proteins (GAPs). In addition, these two GAP segments are linked by a hinge domain, a Rho GTPase binding domain (H/RBD). Numerous proteins and members of small GTPases have been shown to interact with the Plexin cyto-domains and activate diverse pathways, which directly or indirectly lead to dynamic cytoskeleton and actin assembly and the change of cellular morphology (*30*, *40*).

Class 3 Semaphorins, including Sema3A, need to bind with signaling receptors, type-A Plexins (PlxnAs), and their obligated binding partner, Neuropilins (Nrps), to

transduce diverse cellular responses. Neuropilin is a coreceptor which is essential for class 3 secreted Semaphorins signaling by forming a complex with type-A Plexins. Takahashi and colleagues have shown that Sema3A-induced axon repulsion only happens when Neuropilin/Plexin holoreceptor is presented together (*41*). Neuropilin is a transmembrane protein with multiple extracellular domains that are capable of interacting with a variety of proteins including Sema3A (*42*). Interestingly, the C-terminal of Neuropilin is extremely short and barely extends to the cytoplasm. Thus, the general consensus is that Sema3A-mediated cellular response activated by Plexin-A4 (PlxnA4) intracellular signaling, which Neuropilin 1 (Nrp1) plays a crucial role as the obligate coreceptor to link both Sema3A ligand and the PlxnA4 signaling receptor (*2, 43*) (Figure 3).

1.4 Semaphorin 3A/Neuropilin-1/Plexinn-A4 induced diverse cellular responses

Nrp1/PlxnA4 signaling pathway is activated by Sema3A and mediates diverse cellular responses in cortical neuron dendrite morphogenesis and dorsal root ganglion (DRG) growth cone collapse examined *in vitro* and *in vivo* conditions (*2, 12, 44*). Previously, Tran and colleagues showed *in vivo* that Nrp1 (Sema-), which is incapable of binding Sema3A, or PlxnA4-/- mutant mice, cause a significant decrease of basal dendrite in layer V pyramidal neurons. By contrast, Yaron and colleagues showed *in vivo* that PlxnA4-/- or PlxnA3/PlxnA4 double knockout exhibited aberrant DRG sensory neuron axonal projections. Although the list of PlxnA4 intracellular binding protein keeps growing, the mechanism and pathway under the same ligand-receptor complex that mediates diverse cell responses in different types of neuron are still unclear (*30*) (Figure

4). Previous studies showed that PlexinA-mediated axon repulsion is induced by FARP2 (FERM, Rho guanine nucleotide exchange factor [RhoGEF], and pleckstrin domain-containing protein 2) (*11*). FARP2, a Guanine nucleotide Exchange Factor (GEF) protein, further activated Rac1 and Rnd1, small GTPases, and started the signaling cascade. Downstream effectors include R-Ras, PI3K, PTEN, Akt, GSK3β, and CRMP, leading to growth cone collapse and axon repulsion (*30*, *40*). By contrast, the downstream signaling pathway for cortical neuron dendrite outgrowth and branching is not clear. FARP1, a homologue protein to FARP2, which is shown to play a role in Sema6A-PlxnA4 signaling (does not require Nrp1), promotes dendrite length but not branching in the spinal motor neuron of chickens (*45*). Thousand-and-one amino acid 2 kinase (TAOK2), a protein encoded by an ASD susceptibility gene *TAOK2*, may be involved in neocortex basal dendrite formation *in vivo* without affecting apical dendrites (*7*). Taken together, previous studies suggest that PlexinA receptors may associate with different effectors, which could be GEFs or other proteins in different neurons that result in its diverse functions.

1.5 Plexin-A3 and pyramidal neuron spine formation

During neural development, another molecule influencing pyramidal neuron neural connectivity is Semaphorin 3F (Sema3F). Sema3F, a homologue to Sema3A, has been shown to bind Neuropilin2 (Nrp2) that preferentially forms a holoreceptor complex with PlexinA3 (PlxnA3) to mediate a variety of cellular responses in CNS development. Recently, Sema3F has been identified as a negative regulator for pyramidal neuron spine development. Previously, *Sema3F*-/-, *Npn2*-/-, and *PlxnA3*-/- mutant mice have been

shown to display aberrant spine density and size on apical dendrites of layer V cortical neurons (*2*). In addition, Sema3F mRNA has been shown to be a downstream target of the fragile X mental retardation protein (FMRP) (*46*). Thus, understand how Sema3F/PlxnA3/Nrp2 mediate spine formation can help us to reveal how pyramidal neuron connection forms and possibly find a way to prevent the mental disorder.

1.6 Research Objectives

Although previous studies had revealed some parts of Plexin signaling pathways, the mechanisms underlying PlxnA4 signaling and function is still unclear. In this study, I have conducted a structure-function analysis of the PlxnA4 cytoplasmic domain in primary mouse cortical pyramidal neurons. Furthermore, I examined the immediate downstream interaction of Plexin-A4 and the RhoGEF FARP2 in dendrite development. Third, I conducted PlxnA4 ecto-domain analysis in cortical neuron. Lastly, in order to examine pyramidal neuron spine development in a future study, I generated Plexin-A3 cytoplasmic domain deletions mutants, analogous to the Plexin-A4 mutants.

Hypotheses:

1. Promotion of dendritic arborization of cortical layer V pyramidal neurons through Sema3A/Nrp1/PlxA4 signaling is dependent upon distinct cytoplasmic domains within PlexinA4.

2. GEFs (FARP1 or FARP2) associate with PlxnA4 and require for cortical neuron dendritic arborization in response to Sema3A.

Chapter II Materials and Methods

I prepared all the buffers and solutions using double distilled water with analytical grade reagent and autoclaved or filtered to sterilize. Buffers and solutions were stored at room temperature unless mentioned otherwise.

2.1 Animals

Wild Type CD1 mice

PlxnA4 Knockout mice

PlxnA3 Knockout mice

Animals were cared for according to the animal use protocols approved by Rutgers University. For the time pregnancies, embryonic day 0.5 (E0.5) is considered at the noon on the day in which the plug was found. In this study, E13.5 time-pregnant mice were used for dissecting and culture layer V cortex pyramidal neurons.

2.2 Cell lines and Plasmids

A. Cell lines

HEK293T Cells: Human embryonic kidney cells (ATCC® CRL-11268)

COS7 Cells: Fibroblast-like cell, derived from monkey kidney (ATCC® CRL-1651)

B. Plasmids

Alkaline Phosphatase (AP) Protein (control)

AP-Semaphorin 3A fusion protein

AP-Semaphorin 3F fusion protein

PlxnA4 variant constructs (provided by Dr. Avraham Yaron)

Backbone: pCAG. All PlxnA4 variants sequences were based on the wild-type mouse PlxnA4 with myc-tagged on its N-terminus and driven by the chicken β-actin promoter. Domains and motifs were annotated as the following: C1- 1267L-1497L, H/RBD-1498V-1653N, and C2 - 1654H-1890S, LVS- 1593-1595, KRK- 1257-1259. The PlenA4 variants were designed as the following (numbers are amino acids in the full length PlxnA4): PlxnA4 FL 1-1890, ΔCT 1-1266, ΔKRK 1-1890 (KRK to AAA), ΔLVS1-1890 (LVS to GGA), ΔCT+ΔKRK 1-1266 (KRK to AAA), ΔCT+ΔTMC9 1-1257, ΔC1 1-1266 + 1498-1890, ΔH 1-1497 + 1654-1890, ΔC2 1-1653, C1 1-1497, H/RBD 1-1266 + 1498-1653, C2 1-1266 + 1654-1890. (Table 1)

PlxnA3 mutant constructs:

Backbone: pcDNA 3.1(-) to pCAG. All PlxnA3 variants were subcloned from pcDNA 3.1 wild-type mouse PlxnA3 with myc-tagged on the N-terminus. Cytoplasmic domains were amplified by specific designed primers (Table 4) and subcloned to pCAG. Domains were annotated as the following: C1- 1325P-1450K, H/RBD-1451G-1651V, C2-1652S-1872S. The PlxnA3 variants were designed as the following (numbers are amino acids in the full length PlxnA3): PlxnA3 FL 1-1872, ΔCT 1-1324, ΔC1 1-1324 + 1451-1872, ΔH 1-1450 + 1652-1872, ΔC2 1-1651, C1 1-1450, H 1-1324 + 1451-1651, C2 1-1324 + 1652-1872 (See Table 2)

2.3 Software and equipment

A. Software

Perkin Elmer Velocity acquisition and analytical software 6.0.1

NIH ImageJ 1.46

Plugin Sholl analysis

Plugin NeuronJ

Adobe Photoshop CS 6.0 (or higher) was used for drawing tracings of neuron processes and adjusted image's contrast.

Adobe Illustrator CS 6.0 (or higher) was used for assembling the figures in this study

GraphPad Prism 5.0 (or higher) was used for the statistical analyses of Sholl analysis, total dendritic length, dendrite Complexity Index (DCI) and axonal length.

B. Equipment

Class II laminar flow hood (clean bench) or sterile tissue culture (TC) hood

Sterile CO_2 incubator

Centrifuge

Lona/Amaxa Nucleofector Device

Dissecting microscope

Dissection tools: Two fine dissection forceps (no. 5), one straight, one with a bent-tip at 45° angle, one pair of micro-scissors, medium size scissors and medium forceps (Fine Scientific Tools)

Confocal microscope and imaging system

MiliQ or any sterile water system

Electrophoresis system

SDS-PAGE system (Bio-rad)

Water bath

2.4 Mammalian cell culture and transfection

A. Reagent and buffer

Dulbecco's Modified Eagle's Medium (DMEM) (Gibco, Life Technologies, CA): Mammalian cell growth media, store at 4°C.

DMEM (+): DMEM plus FBS, 10%, Pen-Strep, 1X. For 500mL of DMEM (+), add 50 mL filtered 100% FBS and 5 mL Pen-Strep to 450 mL DEME, store at 4°C.

Fetal Bovine Serum (FBS) (Gibco, Life Technologies, CA): Serum for cell culture, store at -20°C.

Penicillin-Streptomycin (Pen-Strep) (Gibco, Life Technologies, CA): Antibiotics for cell culture, store at -20°C.

0.5% Trypsin-EDTA (Gibco, Life Technologies, CA): Reagent for dissociation process, store at 4°C once opened, for long-term storage keep at -20°C.

Phosphate buffer saline (PBS) was prepared in the following steps: for 1 liter of 10x PBS. I weighted 12.7g Na_2HPO_4 (9mM), 2.65g $NaH_2PO_4.2H_2O$ (1.7mM), 85g NaCl (1.5M) in the cylinder and added distilled H_2O (dH_2O) to volume 900 mL. All components were stirred until dissolved and the pH was adjusted to 7.4, before filling the total volume to 1 liter with dH_2O.

Lipofectamine 2000 (Life Technologies, CA): Mammalian cell transfection kit

B. Mammalian cell culture

HEK293T cells and COS7 cells were cultured in 10cm culture dish with DMEM (+) media at 37°C, 5% CO2. When cell reach ~100% confluence split cells to maintain cell line or transfection.

1. Pre-warmed Trypsin-EDTA and DMEM (+) growth media.
2. Removed cell culture media and wash cells with 1X PBS gently.

3. Discarded PBS then added 2.5 mL Trypsin-EDTA and incubated in 37°C incubator for 2 minutes.
4. Added 7.5 mL DMEM (+) and pipetted cells up and down to break cell clumps.
5. Used hemacytometer cell counter to plate ~5 x10^6 cells in a new 10cm culture dish with DMEM(+) media up to 10 mL.
6. Approximately, 1:10 dilution of one 10cm culture dish was used for lipofectamine 2000 transfection.

C. Plasmid transfection

Cells were transfected when cells reached 70-80% confluence. Lipofectamine 2000 (Invitrogen) transfect kit was used by fallowing protocol.

1. Prepared 10μg DNA (AP-Sema3A, AP-Sema3F or APtag for protein collection; PlxnA4 mutants and Nrp1 for immune-staining and immuneprecipitation) and 1.5mL DMEM (-) in tube 1; 40 μL Lipofectamine and 1.5 mL DMEM (-) in tube 2.
2. Mixed tube 1 and tube 2 then incubated in RT for 20 mins. Cells were rinsed with PBS twice and added 4-5 mL DMEM (-) incubateed at 37°C for 20 mins.
3. After 20 mins, I removed the DMEM (-) from plate and added DNA/Lipofectamine/DMEM mixture then incubated at 37°C for 5.5 hours.
4. I rescued the cells by replacing the media to DMEM (+) after 5.5 hours.
5. The cells were kept at 37°C incubator for additional 48-72 hours.
6. The media for AP-Sema3A, AP-Sema3F or APtag proteins from the transfected HEK293 cells were collected after 48-72 hours. For cell immuno-staining,

transfected cell were re-suspended by 0.5% Trypsin-EDTA and plated on the coverslip in a12-well plate culture for an additional 48 hours. See section 2.6 A. Immunocytochemistry for detail. For protein expression and interaction, see section 2.6 B: CO-Immunoprecipitation and C: Western blot.

7. The collected AP-conjugated media were concentrated using Amicon Ultra-15 (Millipore). Protein concentration was determined by AP activity assay using AP substrate buffer- Para-nitrophenyl phosphate (Sigma). AP-tagged proteins were stored in aliquots at -80°C.

D. siRNA knockdown

For siRNA transfection: I followed the methods above used the Lipofectamine 2000 transfect kit. I created an RNase free environment and used RNase free tips. Cells were cultured for an additional 48 hours after transfection and then lysed for CO-IP and Western blot experiments.

2.5 Primary cortical neuron culture and transfection

A. Reagent and buffer

Neurobasal medium (+) (Gibco, Life Technologies, CA): Neurobasal media were stored at 4°C until use. For a total of 125 mL Neurobasal (+): 120 mL Neurobasal media was mixed with 2.5 mL B27 supplement (2% final conc.), 1.25 mL 100x PenStrep (1x final conc.) and 1.25 mL 100x Glutamax (1x final conc.)

HBSS (Hanks balanced salt solution) (Gibco, Life Technologies, CA): Buffer for dissociation process.

L-15 medium (Leibovitz) (Gibco, Life Technologies, CA): Medium for dissection and stored at 4°C.

0.5% trypsin-EDTA

Poly-D-Lysine (Sigma): Make poly-D-lysine at final concentration 0.1 mg/mL in sterilized MiliQ water. Store at 4°C.

DNAse I dissociation solution: Dissociation buffer was used to dissociate cortical neurons to single cell. I prepared 10mL DNAse I dissociation solution and stored at -20°C. I took 9 mL of HBSS in a clean 15mL conical tube and added 400 μL of 10 mg/mL soybean trypsin inhibitor (0.4 mg/mL final conc.), 500 μL of 5 mg/mL DNAse I from Collaborative Research (0.25 mg/mL final conc.), 100 μL of 30% BSA (Sigma for tissue culture) (0.3% [3 mg/mL] final conc.) and 120 μL of 1 M $MgSO_4$ (12mM final conc.)

Cover glasses (VWR): 18mm cover glasses. The cover glasses were placed into a glass beaker for acid wash. The cover glasses were soaked in Nitric acid (70%) for 5-7 hours and the replaced with dH_2O over night. On the second day, I washed the cover slips under running dH_2O for one hour then stored in 100% ethanol at room temperature in the TC hood. Before use, I washed twice with sterile MiliQ water and once PBS in the hood.

Sterile glass Pasteur pipettes

Lonza Nucleofector Kit for mouse neurons

B. Preparation for embryonic cortical primary neuron cultures

1. I prepared Neurobasal (+) media fresh for each culture and placed in TC hood until ready to use.

2. I coated poly-D-lysine on the cover glasses by placing one glass cover slip in each well of 12-well tissue culture dish. Rinsed twice with sterilized MiliQ water and once with 1x sterilized PBS. Added 400 μL/well of poly-D-lysine (0.1mg/mL) to each well and incubated at 37°C for 3-4 hours before plating neurons.
3. I placed DNAse I dissociation solution and plasmids for transfection on ice at the beginning of each culture.
4. I took L-15 media and poured into 10 cm petri dish, a 60 mm petri dish and 1mL into a 1.5mL Eppendorf tubes, and put everything on ice.

C. Dissection in sterile tissue culture (TC) hood

1. Layer V cortical neurons are dissected and cultured form timed-pregnant female mouse on E13.5. I removed the uterine sac from pregnant mouse onto a 10 cm petri dish with L-15 media on ice. For each embryo, I removed the placental sac and placed the embryo on a small petri dish and viewed under the dissect microscope.
2. On ice: I carefully separated the head and body, peel off skin and skull from the back of the dorsal brainstem and work your way rostral toward the cerebral hemispheres (Figure 5)
3. I transferred each dissected cortices into a 1.5mL Eppendorf tube with L-15 media and kept them on ice until all desired cortices were dissected.
4. After all cortices were dissected and collected, I removed the L-15 media and replaced with 1.0mL of 0.5% trypsin-EDTA. Incubated at 37°C for 10 minutes.
5. I took the two sterile 15mL conical tubes and added 9 mL off HBSS into each tube.

6. I transferred the cortices in trypsin into the 15mL tubes with HBSS. Centrifuge the tubes at 1.0x1000g for 5 minutes at room temperature.
7. After centrifugation the tubes were brought back into the TC hood, I carefully aspirated off the HBSS and repeated HBSS wash. The cortices were spun down at 1.0x1000g for 5 minutes at room temperature.
8. While waiting for the centrifugation, I polished two sterile glass Pasteur pipettes to reduce the tips by 50%.
9. I aspirated off the HBSS after the second wash and added 1 mL of DNAse I dissociation solution into the 15 mL tubes and used the polished sterile glass Pasteur pipette and a plastic bulb to gently dissociate the cortices manually.
10. After the manual mechanical dissociation step, I washed the neurons with HBSS and centrifuged at 1.0x1000g for 5 minutes at room temperature.
11. I carefully aspirated off the HBSS and repeated HBSS wash. I centrifuged the dissociated neurons at 1.0x1000g for 5 minutes at room temperature.
12. I aspirated off the HBSS and added 1-3mL of Neurobasal (+) media into the 15mL tube. I took 10 μL of the neurons suspended in Neurobasal (+) media, transferred to a cell counter to estimate the cell number, and plated.
13. After calculating the desired density for plating, I plated 1mL of media + neurons in each well of the 12-well tissue culture plate (containing the poly-D-lysine coated glass coverslips). I incubated the neurons at 37°C in the 5% CO_2 incubator for at least 4-6 hours (up to 12 hours) and changed to fresh Neurobasal (+) media. The media was changed every 48 hours.

14. For dendritic development, neurons were stimulated with 5nm AP-Sema3A or AP protein only at DIV 5 for additional 24 hours.

D. Lonza/Amaxa Nucleofector transfection

1. For primary neuron transfection using the Nucleofector kit (Lonza/Amaxa) for mouse neurons, I prepared 5 µg of expression plasmid containing myristoylated-GFP DNA or DNA of interested in a sterile 1.5mL Eppendorf tube.
2. I aspirated the HBSS after the final wash and added ~0.5-1.0mL of new HBSS into 15mL tube for cell count estimation. Per instructions from the manufacturer, optimal transfection efficiency is achieved with ~2 million cells per transfection. I diluted the dissociated neuron accordingly in a new sterile 15mL tubes and centrifuged to pellet the cells.
3. I added 100 µL of "activated" transfection solution per transfection/DNA construct to each of the dissociated neuron pellets and mixed by pipetting up and down 3-4 times.
4. I transferred the dissociated neurons with transfection solution into each 1.5mL tube containing the GFP DNA or DNA of interest, mixed by pipetting up and down 3-4 times.
5. I transferred the entire mixture into an individual cuvette (included with the kit) and electroporated with the Nucleofector device using the pre-set protocol for mouse neurons.
6. After electroporation, I rescued with 1 mL of Neurobasal (+) media to each cuvette.

7. I used the transfer pipette (included with the kit) to transfer all the electroporated neurons from each cuvette into new sterile 15mL tubes with Neurobasal (+).
8. I plated the transfected neurons at the desired density (~1*10^4 cells/cm^2). Incubated the neurons at 37°C in the 5% CO_2 incubator for at least 4-6 hours (up to 12 hours) and changed to fresh Neurobasal (+) media. Then change media every 48 hours.

E. SiRNA knockdown

For SiRNA transfection: I used the same protocol of Lonza/Amaxa Nucleofector transfection. I created an RNase free environment and used RNase free tips. Neurons cultured additional 48 hours after transfection and then lysed for CO-IP and Western blot experiments or cultured for 6 DIV for dendritic measurement.

2.6 Molecular methods

A. Immunocytochemistry (ICC) staining for primary neurons/COS7 cells

For analyzing aspect of neuronal dendritic morphological development or COS7/neuron cell membrane bound receptor expression detection, cultured neurons or cells were treated with AP-Semaphorin proteins and fixed with 4% paraformaldehyde and stored at 4°C until immunocytochemistry. .

Reagent, buffer and antibodies

4% Paraformaldehyde, PFA (Sigma) was made in PBS, and store at -20°C until use.

PBS-Azide: Add 5% filtered Sodium Azide (made in dH_2O) into 1x PBS to final concentration 0.1%.

Normal donkey serum (NDS, Jackson ImmunoResearch): Aliquots and stored at -20°C.

10% TritonX-100 (Sigma): I took 5 mL of TritonX into 45mL of dH_2O and mixed with a magnetic stir until dissolved completely.

Blocking solution: 1xPBS with 5% NDS and 0.1% TritonX.

Primary antibody solution: I diluted the primary antibody in blocking solution

Secondary antibody solution: I made the secondary antibody dilutions in 1xPBS with 0.1% TritonX.

Mounting media (Vectashield)

Primary antibodies used: monoclonal mouse Myc (D9 hybridoma, DSHB, 1:1000; or 9E10, Sigma, 1:1000), polyclonal rabbit Myc (1:200, Santa Cruz Biotechnology, 1:500), polyclonal rabbit MAP2 (1:1000, Cell signaling), monoclonal mouse GFP (1:800,Invitrogen-Molecular Probes), polyclonal rabbit GFP (1:500, Millipore), mouse monoclonal SMI312 (1:500, Covance), and polyclonal rabbit FARP1 (Santa Cruz Biotechnology, 1:500), monoclonal mouse FARP2 (Santa Cruz Biotechnology, 1:1000).

Secondary antibodies used: AlexaFluor 488 donkey anti-mouse immunoglobulin G (IgG) (1:500, Jackson ImmunoResearch), AlexaFluor 568 donkey anti-mouse (1:1000, Molecular Probes), AlexaFluor 568 donkey anti-rabbit (1:800, Molecular Probes) and Cy3 donkey anti-rabbit (1:800, Jackson ImmunoResearch).

Experiment procedure

1. I aspirated off Neurobasal (+) media from each well of the 12-well dish containing the primary neuron or COS7 cells at the appropriate DIV.
2. I incubated the cells with cold 4% PFA for 10-15 minutes at room temperature or 20-30 minutes at 4°C.

3. I washed three times for 5 minutes each with 1x PBS at room temperature, gently rocking on the rotator. I stored the fixed cells at 4°C with PBS-Azide until ready to begin ICC.
4. I rinsed the cells twice with 1x PBS, 5 minutes each.
5. I incubated the cells in blocking solution.
6. I incubated the cells in primary antibody diluted in blocking solution (from step 5) overnight at 4°C.
7. I washed the cells with PBS three times for 5 minutes each at room temperature.
8. I incubated the cells in secondary antibody solution for 1 hour at room temperature, covered with foil.
9. I washed the cells with PBS three times for 5 minutes each at room temperature.
10. I mounted the glass cover slip on a glass slide with mounting medium (Vectashield). I stored the slides in the dark at 4°C overnight, to let excess mounting medium dry, before viewing under microscope.

For membrane bound protein detection, I omitted TritonX in the entire process.

B. CO-Immunoprecipitation (CO-IP)

HEK293T cells or primary neurons were transfected with the appropriate plasmids DNA or siRNA by using Lipofectamine 2000 (Invitrogen). Cells were cultured for an additional 48-72 hours post transfection until I was ready to perform the pull down experiment.

Reagent, buffer and antibodies

Lysis buffer (pH 7.4): 20mM Tris-HCL, 1% Triton X-100 (add before using), 1 mM EDTA, 1mM EGTA, 150 mM NaCl, protease inhibitor cocktails 1X (50X stock solution, Roche, add before using)

Protein G Sepharose beads (GE Healthcare)

Laemmli sample buffer 3x with 10% β-mercaptoethanol

Pull down antibodies used: monoclonal mouse anti-Myc (DSHB, 1:200), mouse anti-HA (Santa Cruz, 1:1000) or mouse anti-Flag (Sigma, 1:1000)

Procedure (all on ice)

1. Cells were wash with cold PBS twice.
2. I aspirated off the PBS and added 1mL/10-cm plate of lysis buffer. I collected the cells into 1.5 mL tube. (use 500 µL for siRNA transfected cells to get higher concentration protein)
3. Sonication to breakdown cells: I sonicated for 1seccond for a total of 10 times then cool down on ice for 1 minute. Repeated the entire process for three times.
4. I centrifuged at 13K rpm for 25-30 minutes at 4°C. The supernatant was transferred to a new 1.5mL tube.
5. While waiting the centrifugation, I washed the protein G beads with lysis buffer three times (low speed spin down), then topped with lysis buffer to the original volume.
6. I added 30µL of pre-washed Protein G beads and pulldown antibody to supernatant then incubated at 4°C on rotor overnight.
7. On the second day, I washed with lysis buffer 5 times (low speed spin down).

8. I added 30 μL 3X sample buffer and boiling for 10 minutes for SDS-PAGE and Western blot analysis.

C. SDS-PAGE and Western blot

Sodium Dodecyl Sulfate-Polyacrylimide Gel Electrophoresis (SDS-PAGE) gel were freshly made in the lab and stored at 4°C till use. Samples were from freshly lysed cells or from Co-IP.

Reagent, buffer and antibodies

SDS-PAGE gel

Running Buffer: 25mM Tris, 192mM Glycine, 0.1% SDS

Transfer Buffer: 25mM Tris, 192mM Glycine, 10% methanol

TBS Buffer: 20mM Tris, 150mM NaCl, pH 8.0

TBS-T: TBS with 0.05% Tween-20

Blocking Solution: 5% defatted milk in TBS-T

Primary antibodies used: mouse anti-Myc (DSHB, 1:200), mouse anti-HA (Santa Cruz, 1:1000), mouse anti-Flag (Sigma, 1:1000), mouse anti-Actin (MP Biomedicals, 1:5000), rabbit anti-FARP1 (Santa Cruz, 1:250), mouse anti- FARP2 (Santa Cruz, 1:250), rabbit anti-PlxnA4 (Abcam, 1:100)

Secondary antibodies used: anti-mouse IgG HRP (GE Healthcare, 1:2000), anti-rabbit IgG HRP (GE Healthcare, 1:2000)

1. Samples were boiled in sample buffer for 10 minutes then load into SDS-PAGE gel for electrophoresis. Gels were ran at 90v constant for 0.5 hours for stacking and additional 1-1.5hours at 120v constant to separate.
2. Standard SDS-PAGE transfer buffer was used to transfer protein onto PVDF membrane (Millipore) constant 30v overnight at 4°C or constant 90v 1.5 hours on ice.
3. Membranes were blocked using 5% blocking solution (Bio-Rad) in 1x TBST at RT for 1 hour or overnight at 4°C.
4. Membranes were then incubated in primary antibodies over night at 4°C.
5. Blots were washed 3 times 10 minutes each with TBST then incubated with secondary antibody for 2 hours, covered with foil.
6. Then blots were washed 3 times 10 minutes each with 1x TBST. Immunoblots were developed using anti-mouse or anti-rabbit IgG HRP (GE Healthcare, 1:2000) followed by detection with chemiluminescence (Pierce).

D. Molecular cloning

Mouse PlxnA3 cytoplasmic domain (C1, H/RBD or C2) sequence was amplified and subcloned to expression vector: pCAG. Primers were specific designed and used in this study (IDT) (see Table 3). PlxnA3 extracellular domain from pcDNA3.1 (-) was digested and ligated with cytoplasmic domain in pCAG.

1. I amplified the specific PlxnA3 domain with PCR reactions.
2. PCR products were cleaned up by using SpinPrep PCR clean-up kit (Novagen), I followed the protocol in the manufacture’s manual.

3. After clean up, the PCR products and cloning vector were digested with the appropriate restriction enzymes (Fermentas or New England Biolabs) in 37°C for 3.5 hours.
4. The digested product underwent electrophoresis in 0.8% gel and I performed DNA extraction using QIAEX II gel extraction kit (Qiagen).
5. I ligated the vector and DNA fragment with the ligase enzyme overnight at 16°C.
6. Ligation products were transformed in *E.coli* strain DH5α competent cells (Invitrogen) and plated on LB agar plates with carbenicillin (100 µg/mL) incubate in 37°C overnight.
7. I screened the colonies and extract plasmid DNA via NucleoSpin® Plasmid Kit (Macherey-Nagel).
8. All plasmids were first validated with restrict enzyme digest to check the insert and vector size, and then sequenced (Genwiz) to confirm the DNA sequence.
9. I sequence validated plasmids were amplified with Maxi-culture prep. (Qiagen), where I followed the protocol from the manufacture's manual and stored the DNA at -20°C.

2.7 Imaging and data analysis

For each experimental condition/parameter, a total of 30-50 neurons (n) were analyzed from 6-12 independent cultures dissected from 6-9 embryos, taken from 3-plus timed pregnant mice.

A. Confocal microscopy

Z stack confocal images were taken from immunofluorescence stained neuron or mammalian cell cover slips. I compiled confocal Z stack data images then export to high resolution tif files for analysis.

B. Sholl analysis

Sholl analysis was performed using the NIH ImageJ and Sholl Analysis Plugin (http://www-biology.ucsd.edu/labs/ghosh/software/), with the center of all concentric circles defined as the center of cell soma. Sholl analysis parameters are as follows: the smallest radius was 10 μm, the largest radius was 60 μm, and the interval between consecutive radii was 5 μm. For each condition/parameter analyzed, a total of 45-50 neurons, from 6-12 independent cultures, were used to calculate the dendritic intersection number per radii and averaged (Figure 6A). An example of measurement is shown in Figure 7.

I downloaded the Sholl analysis plugin and installed to ImageJ.

1. I took the confocal images under Photoshop and carefully draw the dendrites tracing based on the images. I saved the traced images in gray scale because Sholl analysis plugin requires grey scale image.
2. I opened the traced image in ImageJ, pre-set the scale parameter by clicking “Analyze → set scale”
3. Selected the “point” to indicate soma center
4. Started the analysis by clicking “Plugins → Sholl analysis”. Parameter option will show up, clicked “OK” to start.
5. Numbers of dendritic intersections were saved and recorded for statistical analysis.

C. Total dendritic length and Dendrite Complexity Index (DCI)

The total dendritic length was measured using the ImageJ plugin NeuronJ (http://www.imagescience.org/meijering/software/neuronj/), calculated in microns (μm) for, at least, 35-45 neurons, from 6-12 independent cultures, per condition/parameter. Dendritic order is defined as follows: primary dendrites were traced from the cell soma to the tip of the entire dendritic length, and secondary and tertiary dendrites were traced from the tip to the dendritic branch point using Adobe Photoshop CS6 software. Dendrite lengths that were less than the diameter of the cell soma should be disregarded. The DCI measured by the following formula:

$$\mathrm{DCI} = \frac{\sum \ branch\ tip\ orders \ + \ \#\ branch\ tips}{(\#\ primary\ dendrites)(total\ dendrite\ length)}$$

(*47*) (Figure 6B, 7).

1. I downloaded the NeuronJ Plugin and installed to ImageJ.
2. I opened NeuronJ Plugin by clicking “Plugins →NeuronJ”
3. I opened the traced images from NeuronJ plugin.
4. I started to trace the dendrites by adding tracing manually at beginning and the end of interested dendrite. The program will trace the dendrite automatically.
5. Measure the dendrites by clicking “ measure tracings”

I saved and recorded the dendrite length and manually counted the dendrite numbers.

D. Axon length

The axonal length was measured using the ImageJ with plugin NeuronJ, calculated in microns for a total of 10-15 neurons per construct and across all genotypes. Cortical neurons cultured for 6 DIV, followed by a short treatment (1.5hr) or long treatment (24-

30hrs) of 5nM of AP-Sema3A followed with ICC. Only axons expressing both SMI312 and Myc from neurons resembling pyramidal morphology were used for measurements.

E. Data analysis

Adobe Photoshop CS6 (or higher) was used for drawing tracings of neuron processes. GraphPad Prism 5 (or higher) software was used for the statistical analyses of Sholl analysis, total dendritic length DCI and axonal length. ANOVA followed by post-hoc Tukey test and Student's T test were used in this study.

Chapter III Result

3.1 Specific Plexin-A4 cytoplasmic domains regulate cortical pyramidal neuron dendrite elaboration

3.1.1 Plexin-A4 mutants expressed as Sema3A receptor

To answer our ultimate question, why can Sema3A/Nrp1/PlxnA4 mediate diverse neuronal responses, our collaborator generated several PlxnA4 mutants (see Materials and Methods and Table 1 for details) to perform functional analysis. These constructs are Myc-tagged on the N-terminus and contain different truncated cytoplasmic domains. Expression of mutant constructs needed to be confirmed before their introduction into neurons and examination of the phenotype. First, the constructs were transfected into HEK293 cells and the expressed protein was analyzed using Western blot. Second, co-immunoprecipitation (CO-IP) was used to examine the constructs for their binding affinity with the co-receptor Nrp1. Lastly, the constructs were transfected into cortical neurons to test their ability to insert into the cell membrane as receptors.

The PlxnA4 constructs were first transfected into HEK293 cells for a Western blot protein expression assay using an anti-Myc antibody against Plexin. As shown in Figure 8A, PlxnA4 proteins were expressed in comparable levels. This result indicated that PlxnA4 constructs were expressing the correct protein, as detected by an anti-Myc antibody.

Next, I tested the interaction between PlxnA4 and its obligate co-receptor, Nrp1. Specifically, it was determined whether the binding affinity between PlxnA4 and Nrp1 changes after modifying the cytoplasmic domain. From the protein structure perspective, given that we altered the Plexin structure via mutation or truncation of one or multiple

domains, the structure may have changed, altering the binding affinity. Such changes may then block the signaling pathway. To test for this possibility, I co-transfected the Plexin variants and Nrp1 into HEK293 cells cultured in DMEM (+) media for 48 hours. The cells were then lysed for CO-IP and Western blot analyses following the protocol described in the Methods section. The data showed that binding was observed in PlxnA4 variants, even for the most truncated construct, ΔCT (Figure 8B). This result strongly suggests that the interaction between modified PlxnA4 and Nrp1 was not changed. The morphological alteration, if any, is therefore due to the blocking of the downstream signaling pathway.

Lastly, the variants were transfected into pyramidal cortical neurons to determine surface expression. As observed in Figure 8C, all of the constructs were detected on the neuronal surface without the use of Triton-X in the staining procedure. This result indicates that these PlxnA4 constructs were successfully transfected and able to express on the cell membrane where the original PlxnA4 receptor is located. Taken together, these PlxnA4 constructs expressed correctly and exhibited unchanged binding activity with Nrp1. These constructs were then ready to be introduced into neurons for the examination of domain function.

3.1.2 Plexin-A4 controls cortical neurons dendritic outgrowth and branching

To further test the signaling and function of PlxnA4 in the described system, I examined whether re-introducing full-length PlxnA4 to PlxnA4 KO neurons rescued the dendritic elaboration. Previous literature has shown that these PlxnA4-lacking neurons do not respond to Sema3A stimulation (*2*). The in vitro culture system allowed me to test the

rescue of PlxnA4 function. Moreover, these PlxnA4 KO neurons allow me to define the minimal requirement of cytoplasmic domains to restore signaling function.

The dissociated KO neurons were taken from E13.5 mouse embryos and were transfected with full length PlxnA4 or GFP and cultured in Neurobasal media for 6DIV. At day 5, the neurons were stimulated with 5 nM Sema3A or an AP control for an additional 24 hours. The neurons were fixed with 4% PFA and double labeled with immunofluorescent anti-Map2 (red, dendrite) and anti-Myc (green, plexin) or anti-GFP (green) antibodies. The result showed that only the neurons overexpressing full-length PlxnA4 with Sema3A treatment exhibited restored dendritic elaboration (Figure 9A). The neurons that were transfected with GFP or only stimulated with the AP control were not able to promote dendrite growth. The quantification of more than 35 neurons was performed using Sholl analysis, and both total dendritic length and DCI were significantly decreased in these neurons compared to neurons transfected with PlxnA4 FL and stimulated with Sema3A (Figure 9B-D). These results suggest that re-introducing PlxnA4 can functionally re-establish the dendrite outgrowth phenotype in PlxnA4-null neurons. These data also indicate that the exogenous Sema3A stimulation is necessary for signaling and promoting dendrite elaboration.

3.1.3 Plexin-A4 C1 and H/RBD domains are necessary for dendrite elaboration

To examine which protein domain is regulating the observed effect, I transfected PlxnA4 constructs to KO neurons and analyzed their phenotypes. As shown in Figure 10-1A, ΔCT-transfected neurons were unable to rescue dendrite growth and branching. Interestingly, the ΔC1 domain- and ΔH/RBD domain-transfected neurons resulted in no

or very little rescue in KO neurons. In contrast, ΔC2 domain-transfected neurons fully rescued the dendrite phenotype. Quantifying all three methods of measurement for dendrite, I found dramatic decreases in the ΔCT-, ΔC1-, and ΔH/RBD-overexpressing neurons. However, ΔC2-transfected neurons showed no significant difference compared to the FL PlxnA4-transfected neurons (Figure 10-1B-D). This result suggests that the C1 and H/RBD domains are both important for dendrite arborization in cortical neurons given that only ΔC2-transfected neurons were able to rescue the dendrite branch and growth.

Furthermore, using the same method, neurons that were transfected with single cytoplasmic domain (C1, H/RBD or C2 only) were unable to rescue the dendrite elaboration phenotype (Figure 10-2A). Interestingly, neurons transfected with C1 or H/RBD alone exhibited higher dendritic intersection numbers, dendritic lengths and DCI than neurons transfected with C2 alone (Figure 10-2B-D). This effect might be due to the C1 and H/RBD domain being involved in promoting dendrite growth and branching or the C2 domain inhibiting function. Taken together, the results suggest that the C1 and H/RBD domains must both be present to respond to Sema3A stimulation and fully promote dendrite growth. The data also suggest that the Sema3A/Nrp1/PlxnA4-mediated dendrite promotion is controlled by specific PlxnA4 domains.

3.1.4 Plexin-A4 overexpression in WT cortical neurons

After examining the effects of PlxnA4 mutant receptors in KO neuron, I further examined the gain-of-function effects of these mutant receptors in wild-type cortical neurons. Upon overexpressing PlxnA4 FL, confocal imaging and dendrite quantification showed that these neurons were similar to the GFP-transfected neurons following

treatment with Sema3A (Figure 11). In contrast, neurons without Sema3A treatment exhibited low dendrite branching and length. This result suggests that PlxnA4 overexpression did not increase dendrite length and branching. That is, no gain-of-function was observed when the construct was overexpressed in cortical neurons. This effect may be due to the limited number of endogenous Nrp1 co-receptors in neurons (Figure 12). Specifically, the overexpressed PlxnA4 and the endogenous receptor must compete with Nrp1 to form a functional complex. Only the Nrp1/PlxnA4 complex together with Sema3A can activate the downstream pathway.

After confirming that there was no gain-of-function due to the overexpression of PlxnA4 FL, I tested the effects of the mutant constructs in the neurons. As expected, the ΔCT-, ΔC1-, and ΔH/RBD-transfected neurons showed a significant decrease in the dendrite length and complexity (Figure 13-1A). In contrast, ΔC2-transfected WT neurons exhibited a similar dendrite profile as the FL-transfected neurons after Sema3A treatment. These results support our previous PlxnA4 KO data that the C1 and H/RBD domain are involved in and required for the promoting dendrites. Interestingly, neurons transfected with the H/RBD domain alone exhibit a partial response to Sema3A stimulation based on Sholl analysis. In contrast, neurons transfected with C1 or C2 alone retain low intersection numbers (Figure 13-2). This result is consistent with the PlxnA4-/- finding that Sema3A-mediated cortical neuron dendrite elaboration occurred via the C1 and H/RBD domains. Taken together, these findings suggest that the activity of the Nrp1/PlxnA4 functional complex is limited by endogenous Nrp1. The overexpression of Plexin does not result in a gain-of-function. Additionally, these results support and validate our complementary in vitro systems.

3.1.5 Plexin-A4 variants do not alter axonal length in cortical neurons

I have shown that Sema3A/Nrp1/PlxnA4 can mediate cortical dendrite branching and growth. As shown in an earlier study, Sema3A signaling can affect cortical neuron axon guidance in vivo (*48*). I therefore considered whether PlxnA4 constructs alter axon development in cortical neurons. To this end, cortical neurons were transfected with the PlxnA4 construct and double-labeled with SMI312 (red, axon) and Myc (green, plexin). In Figure 14, PlxnA4 FL, ΔCT, ΔC1, ΔH/RBD, and ΔC2 constructs are expressed in axonal processes with or without Sema3A treatment. Interestingly, WT neurons overexpressing PlxnA4 constructs did not show significant changes in axonal length (Figure 14B). These data suggest that PlxnA4 constructs alter the dendrite signaling pathway but not axon development in mouse cortical neurons.

3.2 Plexin-A4 intracellular associated protein RhoGEF FARP2 regulates dendrite arborization in cortical neurons

3.2.1 LVS & KRK motifs are necessary for cortical neuron dendrite outgrowth

To further investigate the downstream signaling pathway of Sema3A/Nrp1/PlxnA4 and how it mediates diverse cellular responses, I considered two very important motifs in the Plexin A4 cytoplasmic region, LVS and KRK. As previously reported, many small GTPase members, such as *Rac1* and *Rnd1*, are involved in Semaphorin/Plexin-induced axon guidance (*49–51*). The LVS motif is a conserved GTPase-binding motif in the H/RBD domain throughout the type-A plexin family (shown as LVP in PlxnA1-A3). Moreover, LVS/LVP motifs have been shown to be necessary for axon repulsion and COS cell collapse following Plexin signaling activation. However,

the role of the LVS motif to Sema3A in pyramidal neuron dendrite elaboration remains unknown. Therefore, I tested whether this GTPase binding motif is required for Sema3A-mediated dendrite development. The PlxnA4 LVS motif was mutated to GGA (ΔLVS) with a myc-tag at the N-terminus. I used the same approach as described above to transfect mutant ΔLVS to both E13.5 WT and PlxnA4 KO mouse cortical neurons. As shown in Figure 15A-C, WT neurons transfected with the LVS mutant exhibit a significant decrease in dendrite length, DCI, and intersection numbers, from 10 to 60 μm. Similar to the WT neurons, transfected KO neurons were unable to rescue the dendrite phenotype. The data revealed a strong decrease in the dendrite length, DCI, and Sholl analysis intersection numbers (Figure 15D-F). This result suggests that the small GTPase binding motif is critical for Sema3A-mediated cortical neuron dendrite branching and growth.

Another motif that might be involved in Sema3A/Nrp1/PlxnA4 signaling is the KRK motif. As previously shown, the conserved KRK motif is the binding site for FERM domains. FARP1 and FARP2 are FERM domain-containing GEFs (guanine nucleotide exchange factor). These proteins have been shown to associate with Plexin and to be involved in Semaphorin/Plexin-mediated spinal motor neuron dendrite outgrowth and DRG growth cone collapse (*11*, *45*). I therefore tested whether the KRK motif also promotes cortical neuron dendrite development (the examination of the function of FARP1/2 will be discussed below). The PlxnA4 KRK mutant (ΔKRK) contained a replacement of the basic triplet KRK amino acid sequence to AAA. As observed in Figure 16A-C, the overexpression of KRK mutants competed for Nrp1 with endogenous PlxnA4, causing a strong decrease in dendrite length and branching. All three

quantification measures showed significant reductions compared to FL-transfected neurons. Moreover, the KRK mutant was unable to rescue the dendritic phenotype in PlxnA4 KO neurons following Sema3A treatment (Figure 16D-F). This result suggests that the KRK motif is necessary for cortical neuron dendrite elaboration. Taken together, these experiments indicate that Sema3A-mediated cortical dendrite growth is strictly regulated by LVS, the small GTPase binding motif, and KRK motif, through interactions with downstream regulators.

3.2.2 FARP1 and FARP2 interaction with the KRK motif and juxtamembrane regions

FARP1 and FARP2 are GEFs that are involved in many intracellular cascade pathways, including Plexin-mediated dendrite outgrowth and DRG growth cone collapse. To study the PlxnA4-mediated dendrite promotion signaling pathway, I first examined the binding affinity of FARP1/2 for PlxnA4. FARP2 is a Rac-GEF protein that associates with Plexin-A1(PlxnA1) through the conserved basic amino acid motif, KRK (*11*). However, no clear evidence has shown that FARP2 binds with PlxnA4 through the KRK motif. FARP1 (Rho-GEF), a homologue protein to FARP2, has been shown to interact with PlxnA4, but not A1, via its FERM and PH domains (*45*). Both FARP1 and FARP2 have been shown to trigger downstream signaling: FARP1 promotes dendritic growth in spinal motor neuron through Sema6A/PlexA4; FARP2 binds to the KRK motif on PlxnA1 and causes growth cone repulsion in DRG neuron. This difference in these GEF proteins might explain their opposing functions in Sema3A/Nrp1/PlxnA4 signaling.

Here, I examined whether FARP1 and FARP2 can interact with full length PlxnA4 and the KRK mutant in vitro. HEK293 cells were co-transfected with Myc-

tagged full length PlxnA4 or the KRK mutant with HA-tagged FARP1 or FARP2 for CO-IP. By analyzing the resulting Western blots, I detected that the affinity between FARP2 and the KRK mutant significantly decreased, whereas FARP1 maintained similar affinity (Figure 17A). The quantification of four repeat experiments showed that the FARP2 interaction was reduced by approximately 55% when interacting with the KRK mutant, but no reduction was observed for FARP1 (Figure 17B). This result suggest that FARP2 binds to PlxnA4 through the KRK motif, as shown in a previous study (*11*). However, as the FARP2 and KRK mutant interaction was not completely abolished, the binding is not completely dependent on the KRK motif. In contrast, the interaction between FARP1 and PlxnA4 was not significantly reduced by any single deletion of the PlxnA4 cytoplasmic domain, ΔCT, or mutation of the KRK motif (Figure 17A, C). Two additional PlxnA4 mutants were tested: the ΔCT+ΔKRK construct, which replaced KRK with AAA in the ΔCT mutant; and ΔCT + ΔTMC9, which contained a 9-amino acid deletion that included KRK in cytoplasmic region of ΔCT (see Table 1). Interestingly, the interaction dramatically decreased for both of these constructs (Figure 17D), suggest that FARP1 binding is not limited to the KRK domain. Taken together, the experimental results suggest that two GEFs, FARP1 and FARP2, are both associated with PlxnA4, but with different affinity levels, via the FERM domain and the KRK motif, with the assistance of the juxtamembrane region.

3.2.3 RhoGEF FARP2, but not FARP1, is required for dendrite elaboration

From previous research, it is known that FARP2 is necessary for Sema3A/Nrp1/PlxnA1-mediated axonal repulsion in chicken DRG neurons (*11*).

Alternatively, FARP1 is important for the promotion of dendrite growth in chicken spinal motor neuron via Sema6A/PlxnA4 signaling (*45*). These two opposing functions might be due to their triggering of different pathways in the cell. In this study, Sema3A/Nrp1/PlxnA4 was also found to mediate opposing functions in cortical and DRG neurons. I tested whether FARP1 or FARP2 is responsible for promoting cortical neuron dendrite growth. I therefore used siRNA to knock down FARP1 and FARP2 in primary neurons to test the function of these GEFs in the promotion of pyramidal neuron basal dendrite growth in the context of the Sema3A/Nrp1/PlxnA4 pathway. In this way, I was able to see the effect of a lack of FARP1 or FARP2 in cortical neuron dendrite development.

For these experiments, cortical neurons were co-transfected with siRNA against FARP1 or FARP2 and GFP plasmid, grown for 5 DIV, and then stimulated with 5 nM Sema3A for an additional 24 hours. Western blot analysis showed the FARP1 and FARP2 proteins were knocked down, as expected (Figure 18A). The neurons that were co-transfected with siRNA control showed normal dendrite outgrowth in response to Sema3A (Figure 18B) compared to Sema3A un-treated neurons. Interestingly, FARP2-knockdown neurons showed a dramatic reduction of dendrite elaboration (Figure 18B), while the knockdown of FARP1 did not affect cortical dendrite morphology. Sholl analysis, as well as total dendrite length and DCI quantification, was performed. ANOVA analysis followed by Post-hoc Tukey's test indicated a significant decrease in dendrites in FARP2-knockdown cortical neurons (Figure 18C-D). This result suggests that FARP2 is required for mouse cortical neuron basal dendrite promotion in the cellular level. These

data also suggest that FARP1 does not affect dendrite outgrowth in mouse cortical neurons.

3.3 Extracellular domains of Plexin-A4 control the binding-affinity for Neuropilin-1

3.3.1 Modified extracellular domains of Plexin-A4 variants affect dendrite morphology

The previous cytoplasmic region mutant binding assays showed that all of the modified PlxnA4 constructs had the same interaction with Nrp1. This result suggests the Nrp1/PlxnA4 interaction occurs outside the cell membrane. This is similar to a previous study in which Takahashi et al. showed that PlxnA1, A2, and A3 interact with Nrp1 and Nrp2 in the extracellular region (*41*). To examine the interaction site, extracellularly modified constructs were tested. Three extracellular mutants were tested: ΔSema, from which the extracellular Sema domain is deleted; ΔIg, from which the extracellular Ig domain is removed; and Δecto, from which the entire extracellular portion of PlxnA4 is removed (Table 1). In these experiments, I sought to test which domain(s) is involved in the PlxnA4 and Nrp1 interaction outside the cell membrane. Plexin variants and Nrp1 were co-transfected into HEK cells for 48 hours; the cells were then lysed for Co-IP. The result showed that regardless of the presence of Sema3A, PlxnA4 and Nrp1 binding is unchanged, suggesting that the ligand is not necessary in the holo-receptor interaction (Figure 19A). In the binding assay, Nrp1 was found to bind to the PlxnA4 FL, ΔSema, and ΔIg proteins, but not with Δecto (Figure 19B). This result indicates that the Ig and Sema domains bind and interact with Nrp1 independently. However, when the entire extracellular domain is removed, binding can no longer occur.

Next, I further tested the effect of these three constructs on cortical neuron dendrite branching. The culture experiments showed that ΔIg- and Δecto-transfected neurons had a significant reduction in their dendrite outgrowth (Figure 19C-D). Interestingly, ΔSema-transfected neurons fully responded to Sema3A stimulation. In previous research, the Sema domain PlxnA1 has been shown to auto-inhibit signal transduction, whereas constitutive activation has been observed in Δecto and ΔSema mutants, leading to axon repulsion and growth cone collapse effect (*3*). My results suggest that the PlxnA4 Sema and Ig domains independently interact with Nrp1. Meanwhile, the Sema domain may prevent the activation of PlxnA4, similar to PlxnA1.

3.4 Cloning new Plexin-A3 mutants and testing expression for each mutants

3.4.1 Generation of Plexin-A3 variant constructs

Having identified the required intracellular domains for PlxnA4 signaling and the associated downstream regulators, I further analyzed another signaling pathway. PlxnA3 is another important receptor for Class 3 Semaphorins (especially for Sema3F) in central nervous system development. Similar to PlxnA4 signaling complex, PlxnA3 requires a co-receptor, Nrp2. These proteins bind to form a holo-receptor that responds to Sema3F. To understand the mechanism behind this complex, I constructed new PlxnA3 constructs from a full length PlxnA3 sequence in a pcDNA3.1 backbone (Figure 20). The created PlxnA3 constructs were similar to those used for PlxnA4, i.e., a truncated cytoplasmic region with a myc-tag on the N-terminus. Specific primer sets and restriction enzyme cutting sites were designed for these constructs (See Table 2)

3.4.2 Plexin-A3 mutants express properly on cortical neuron membrane

Before introducing the PlxnA3 constructs into neurons and examining the phenotype, the construct characteristics need to be confirmed. First, the DNA size for each mutant construct was confirmed by restriction enzyme double digestion using NotI and NheI (Figure 21A). The results of this analysis confirmed that each construct was successfully cloned to target the cytoplasmic domain. Next, the constructs were transferred to COS7 for the cell surface expression assay. The transfected COS7 cells were fixed and labeled with an anti-Myc antibody, without the use of Triton-X to prevent opening of the cell membrane during the staining process. Confocal pictures (Figure 21B-J) showed Myc signal on each transfected cell surface. This result suggested that these PlxnA3 constructs were able to express in COS cells and reach the cell membrane to act as a receptor. Furthermore, Western blot results for the PlxnA3 mutants showed that they expressed properly in HEK293 cells (Figure 22A). These constructs were successfully transfected and expressed the truncated PlxnA3 proteins of the predicted sizes. Co-IP experiments also showed that PlxnA3 mutants exhibited high affinity for the co-receptor Nrp2 (Figure 22B, C). Lastly, cortical neurons were transfected with PlxnA3 mutants, which also localized the membrane based on the anti-Myc antibody signal (Figure 22D). Based on these observations, these Myc-tagged PlxnA3 cytoplasmic region deletion constructs were successfully designed, cloned, and expressed proteins of the predicted size. Moreover, these proteins localized, as predicted, to the neuronal cell membrane as receptors. Thus, these constructs could then be used for the next step, namely, PlxnA3 KO dendritic spine phenotype rescue experiments.

Chapter IV Discussion

Previous studies have shown that guidance cues, include Semaphorins, mediate diverse cellular responses by binding to different receptor complexes during development (*28*, *52–55*). Thus, the same molecule can play different roles through a variety of signaling partners and mechanisms, even targeting different population of neurons. However, the mechanisms underlying how the same ligand/receptor complex mediates different cellular responses is unclear (*2*, *14*, *17*, *56*).

In this study, I focused on the signaling mechanism of the guidance receptor PlxnA4 in the following ways: i) analyzing and characterizing the role of different cytoplasmic domains in response to Sema3A; ii) investigating important conserved motifs and GEFs in the signaling pathway. The results of my study suggested that cortical pyramidal neurons require the C1 and H/RBD domains of PlxnA4 to mediate dendritic branching and elaboration in the presence of Sema3A. The data also indicated that the LVS and KRK motifs are involved in the signaling pathway. Analysis of the GEF proteins FARP1 and FARP2 gave different results. While FARP2 is necessary for dendrite outgrowth, FARP1 showed no effect on dendrites in pyramidal neurons. These data together demonstrate that specific cytoplasmic domains and conserved motifs are responsible for pyramidal neuron dendrite arborization. Downstream proteins, such as GEFs, play important roles in triggering the signaling cascade. Thus, further investigation of these downstream effectors will be necessary to complete the story.

Furthermore, I analyzed the PlxnA4 extracellular domain’s interaction with Nrp1 and its effect on dendritic development. The results of this series of experiments suggest

that the Sema and Ig domains may independently interact with Nrp1. Additionally, the Sema domain may play a role in preventing PlxnA4 activation.

Lastly, newly constructed PlxnA3 mutants were evaluated for their characteristics were confirmed to bind their co-receptor. PlxnA3 mutants were ready to test in cortical neurons for spine morphogenesis.

4.1 Distinct cytoplasmic domains mediate neuron dendrite development

Sema3A/Nrp1/PlxnA4 signaling was originally discovered in a study of axonal repulsion. Recent research has shown that Plexins and Semaphorins are involved in different systems, such as cardiovascular development, immune system function, cell migration, and even cancer (*33*–*35*). These studies suggest a flexible signaling ability of the Plexin receptor complex. Yet, the mechanism underlying how the ligand/receptor complex Sema3A/Nrp1/PlxnA4 mediates the opposite neuronal response is not clear. In this study, I showed for the first time that the PlxnA4 cytoplasmic C1 and H/RBD domains are required for promoting mouse pyramidal neuron dendrite outgrowth at embryonic stages. The C2 domain, in contrast, does not affect dendritic arbor and length as no effect was observed upon its deletion (Figure 10-1). Alternatively, Dr. Yaron's lab in Weizmann Institute of Science Israel (our collaborators) showed that the H/RBD and C2 domains are important and trigger DRG neuron growth cone collapse (*57*). Therefore, the same ligand/receptor pair mediated opposing neuronal responses during development via different signaling pathways. In addition, these complementary experiments in DRGs and cortical neurons serve as mutual controls and indicate that PlxnA4 mutants remain functional receptors. For example, PlxnA4 without the C2 domain is sufficient to promote cortical neuron dendrite growth but cannot cause DRG growth cone collapse.

This result indicates that the dysfunction of the mutants was not due to protein mis-folding or a change in protein trafficking given that they can still properly trigger cellular responses in the other system. To further investigate this effect, one further direction will be determine how these different mechanisms are regulated in specific neuronal types. It will be interesting and important to understand whether a dominant pathway or specific molecules are involved and trigger signal transduction.

In addition, previous studies have revealed that the C1 and C2 domain from PlexinA1 and B1 share sequence similarities with Ras GTPase activating proteins (GAPs) (*30, 58*). When the small GTPase Rnd1 is recruited and shown to associate with H/RBD domain on the LVS motif, C1 and C2 display GAP activity to enhance hydrolysis of GTP to GDP, which lead to the switching off downstream signal transduction. Interestingly, while removing the PlxnA4 C2 domain (ΔC2), my data suggest the PlxnA4 variant functions the same as WT and did not lower cortical neuron dendrite elaboration (Figure 10-1, 13-1). Does that mean PlxnA4 mediate cortical neuron dendrite elaboration does not require GAP activity to turn off the signal? The answer is still unclear and three reasons may explain the phenomenon: 1) Unidentified GAPs may exist in the system to help turn off GTPase activity. So far, PlxnAs has been shown to associate with multiple small GTPases (*Rac, Ras, Rnd1*) in the signaling pathway (*30*). In 2012, a RacGAP protein, β2-Chimaerin, has been found to selectively bind to Nrp2 in Sema3F/Nrp2/PlxnA3 system and is necessary for axon pruning in mouse hippocampal dentate gyrus (DG) (*59*). The growing list of Plexin downstream binding effectors may include unidentified GAPs that could help speed up small GTPase hydrolysis. 2) Rnd1 GTPase activity is slowly turned off by self-hydrolysis. Even without GAP activity, small

GTPase can still switch from the on state to the off state by self-hydrolysis at a much slower rate. Although my data suggests there is no significant difference between FL and ΔC2 transfected neurons, it might explain the slightly lowered dendrite growth shown in the data obtained from the ΔC2 construct. 3) C1 domain may display partial Ras GAP activity. Previous studies in the PlxnA1, B1, C1 and D1 show that LRR amino acid motif on the C1 domain and LRF motif on the C2 domain are essential for catalytic activity for Ras GAP (*60*, *61*). When all three Arginines were mutated to Alanine, Plexins failed to display Ras GAP activity. In my experiments, I tested two extra mutants for GAP activity: PlxnA4 ΔRRAA, which only mutates Arginine to Alanine on the C1 domain and PlxnA4 ΔRA, which only mutates Arginine to Alanine on the C2 domain (Figure 23). My data shows PlxnA4 RRAA mutant has lower dendrite elaboration in the WT neurons and is unable to rescue the dendrite phenotype in PlxnA4 KO neurons. The Sholl analysis result of PlxnA4 RRAA is almost identical to the ΔLVS mutant. On the other hand, the PlxnA4 RA mutant shows a partial rescue of the KO neuron dendrite phenotype. According to the data, an LRR motif on the C1 domain may be able to partially display Ras GAP activity. Therefore, these reasons might be able to explain how, while removing the entire C2 domain, the construct is still able to promote cortical neuron dendrite growth and branching. Further GAP activity experiments are still required to determine which reason(s) is/are the real situation.

4.2 Downstream effectors change dendrite arborization

The conserved LVS motif has been shown to closely interact with small GTPases such as *Rac1*, *Rnd1* and *Ras*, in axon guidance. The KRK motif has been shown to bind with the FERM domain in FARP1 and FARP2, which function as GEFs to activate small

GTPases such as *Rac1*. These two motifs have been shown to be important in axonal guidance and neuron development in a non-cortical neuron (*11*, *30*, *45*, *49–51*). No clear evidence shows how the two motifs in PlxnA4 are related to cortical neuron dendrite development. In this study, my data showed for the first time that both the LVS and KRK motifs are required for dendrite morphogenesis in mouse cortical neurons. My results clearly showed that mutating either motif leads to a significant reduction in dendrite length and branching (Figure 15, 16). The mechanism underlying PlxnA4-mediated cortical neuron dendrite promotion most likely begins with activated GEFs, which then trigger the small GTPase exchange mechanism, from GDP to GTP, recruiting another small GTPase then leading ultimately to binding of the H/RBD domain (Fig 21). Further experiments are require to understand the different mechanisms of dendrite promotion and growth cone repelling.

Further investigation of the FERM-containing proteins FARP1 and FARP2 showed that only FARP2 could trigger cortical neuron dendrite outgrowth (Figure 18). FARP1 and FARP2 have previously been shown to bind PlxnA4 and A1, which are involved in DRG and spinal motor neuron development (*11*, *45*). My data demonstrated that these two related GEFs associate with PlxnA4 in a different manner. FARP2 strongly binds to the KRK motif but requires additional sequences in the PlxnA4 cytoplasmic domain to stabilize binding. Alternatively, FARP1 binding is unaltered by mutations in the KRK motif. However, the removal of the entire PlxnA4 cytoplasmic domain, including the KRK motif, abolishes the interaction between FARP1 and PlxnA4 (Figure 17). This effect likely occurs because FARP2 is needed to dissociate from PlxnA4 upon activation; therefore, its binding is looser than that of FARP1, which functions while still bound to

the receptor (*11*). In addition, the KRK motif is located next to the transmembrane domain, which was present in all of the PlxnA4 mutants, including ΔCT. This result suggests that although FARP2 is recruited through the KRK motif, it is insufficient to trigger downstream signaling and generate the cellular response without the cytoplasmic domain(s).

Furthermore, recent research has demonstrated FARP1 to be involved in regulating excitatory synapse number and spines by acting through GTPase *Rac1* and the downstream synaptogenic adhesion molecule SynCAM1 (*62*). Thus, whether FARP1 will play a role in dendritic differentiation or dendritic remodeling at a later developmental stage still needs to be examined. In addition, there may be other unknown FERM-domain containing proteins that interact with PlxnA4 through KRK and that affect cortical neuron dendrite growth and branching. Future experiments, such as protein mass spectrometry, are necessary to investigate and analyze the specific downstream signaling effectors that are involved in the dendrite elaboration pathway.

4.3 Signaling pathway is highly regulated by Ectodomains

Sema3A mediates neuronal responses that require Nrp/PlxnA as holoreceptors (*63*). Previous studies have shown that PlxnA1 interacts with Nrp1 mainly in the ectodomains. Upon deleting the extracellular domain, binding between PlxnA1 and Nrp1 was abolished (*3*). However, no published evidence has defined an interaction site between PlxnA4 and Nrp1 in mouse cortical neurons. In my study, all of the cytoplasmic domain mutants were still able to interact with Nrp1 (Figure 8).Moreover, my preliminary data showed that both the Sema and Ig domains could independently interact with Nrp1. However, when the ectodomains were completely deleted, no interaction was detected with Nrp1 in the

Co-IP assay (Figure 19). This result is similar to the previous PlxnA1 model, suggesting that PlxnA4 may interact with Nrp1 in a similar manner (*3*). My data also support the previous Nrp structure data, specifically, that binding between Nrp and PlxnA involves the interaction multiple domains (*42*). More recently, a crystalized structure showed Nrp1 bridging the Sema domain of Sema3A and PlxnA2 and stabilizing the heterotrimer complex (*43*). Together, these data suggest that the extracellular domain interaction is highly regulated and necessary for the receptor recruiting the correct binding partner. Without the Nrp1 binding to PlxnA4, Sema3A-mediated dendrite promotion would not occur.

Furthermore, Takahashi et al. indicated that PlxnA1 is autoinhibited by its own Sema domain (*3*). Upon removal of the Sema domain or entire ectodomains, PlxnA1 is constitutively active and induces growth cone collapse. Interestingly, my data showed that only the PlxnA4 ΔSema mutant leaves dendritic arborization unchanged in the presence of Sema3A, whereas the ΔEcto and ΔIg mutants cannot promote dendrite growth. No constitutive promotion of dendrite growth occurs in the ΔEcto mutant (Figure 19). This difference likely occurs because dendrite promotion and growth cone collapse act through different pathways. Although the Sema domain may autoinhibit PlxnA4 activation, the PlxnA4 ΔSema mutant is not fully functional in triggering dendritic arborization in cortical neurons. Further experiments on PlxnA4 KO neuron rescue without Sema3A treatment are needed to investigate the Sema domain's autoinhibition of PlxnA4. Additionally, the crystal structure of the receptor complex is also required to reveal the details of the binding between the ligand and holoreceptor.

4.4 Plexin-A3 mutant may unveil the pathway of dendritic spine formation

PlxnA3 is a membrane-bound receptor that has been shown to interact with Sema3F/Nrp2 to mediate cortical neuron dendritic spine inhibition and regulate hippocampal axonal projection (*2*, *64*). Dr. Tran's data showed a similar aberrant spine phenotype in Nrp2 KO mice and Sema3F KO mice. In addition, the preliminary behavioral data from Nrp2 KO mice in our lab are consistent with Dr. Shiflett's results showing these mice to be lacking in instrumental learning ability. Furthermore, recent research also indicated that Fragile X syndrome mice have an increased number of immature spines and synapses in pyramidal neurons (*65*, *66*). Fragile X syndrome is a common inherited mental retardation disorder. When the *FMR1* gene, which encodes the fragile X mental retardation protein (FMRP), is absent or mutated, Sema3F mRNA cannot unwind, possibly lowering Sema3F translation (*46*). Therefore, it is possible that the PlxnA3 pathway does not activate and lead to an aberrant spine phenotype. Based on the available data, PlxnA3 shows the ability to regulate cortical neuron spine formation and hippocampal axon projection, effects that may be closely related to learning and memory function. Like PlxnA4, the downstream signaling pathway of Sema3F/Nrp2/PlxnA3 in the context of neural development has not been clearly defined. Here, I began this analysis by cloning new PlexA3 mutants and validating the features of the expressed protein. I will next be able to perform functional analyses to define the mechanisms underlying how Sema3F/Nrp2/PlxnA3 inhibits spine morphogenesis.

Figure 1.

Figure 1. Confocal image of wild-type (WT) E13.5 mouse primary cortical neuron Neuron stained for both Myc (for PlexinA4, green) and SMI-312 (panaxonal neurofilament marker, red). Scale bar, 20 µm.

Figure 2.

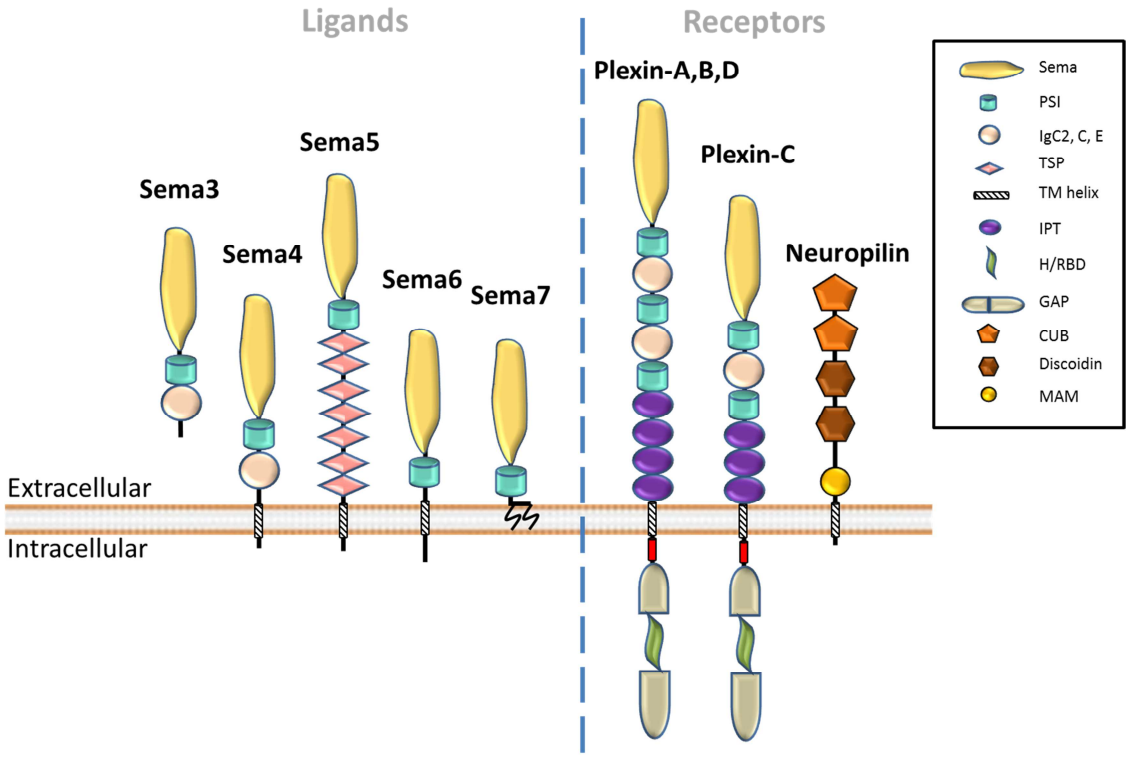

Figure 2. Schematic representation of Semaphorins and their receptors

Here showed five classes of vertebrate Semaphrins and the major holoreceptor complex required for Semaphorin mediated neuronal responses. Only class 3 Semaphorins in vertebrate are secreted form Kolodkin *et al*. (*9*)

Figure 3.

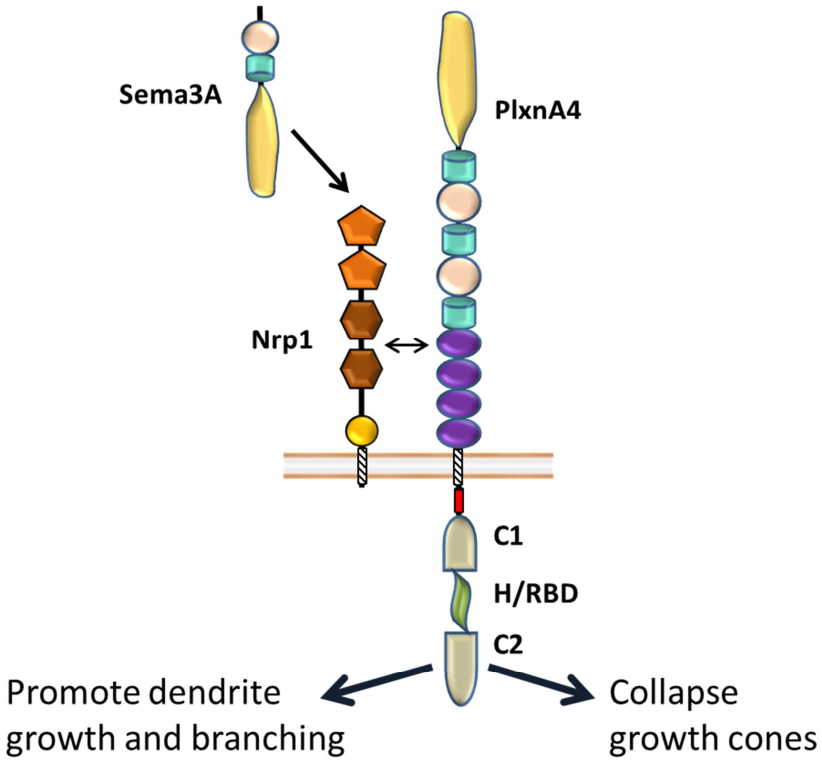

Figure 3. Schematic receptor complex for Sema3A

Nrp1 is the obligate binding receptor for Sema3A. PlxnA4 and Nrp1 forming holoreceptor and signal diverse cellular responses through intracellular domains: C1, H/RBD and C2. Figure modified form Kolodkin *et al*.(*9*)

Figure 4.

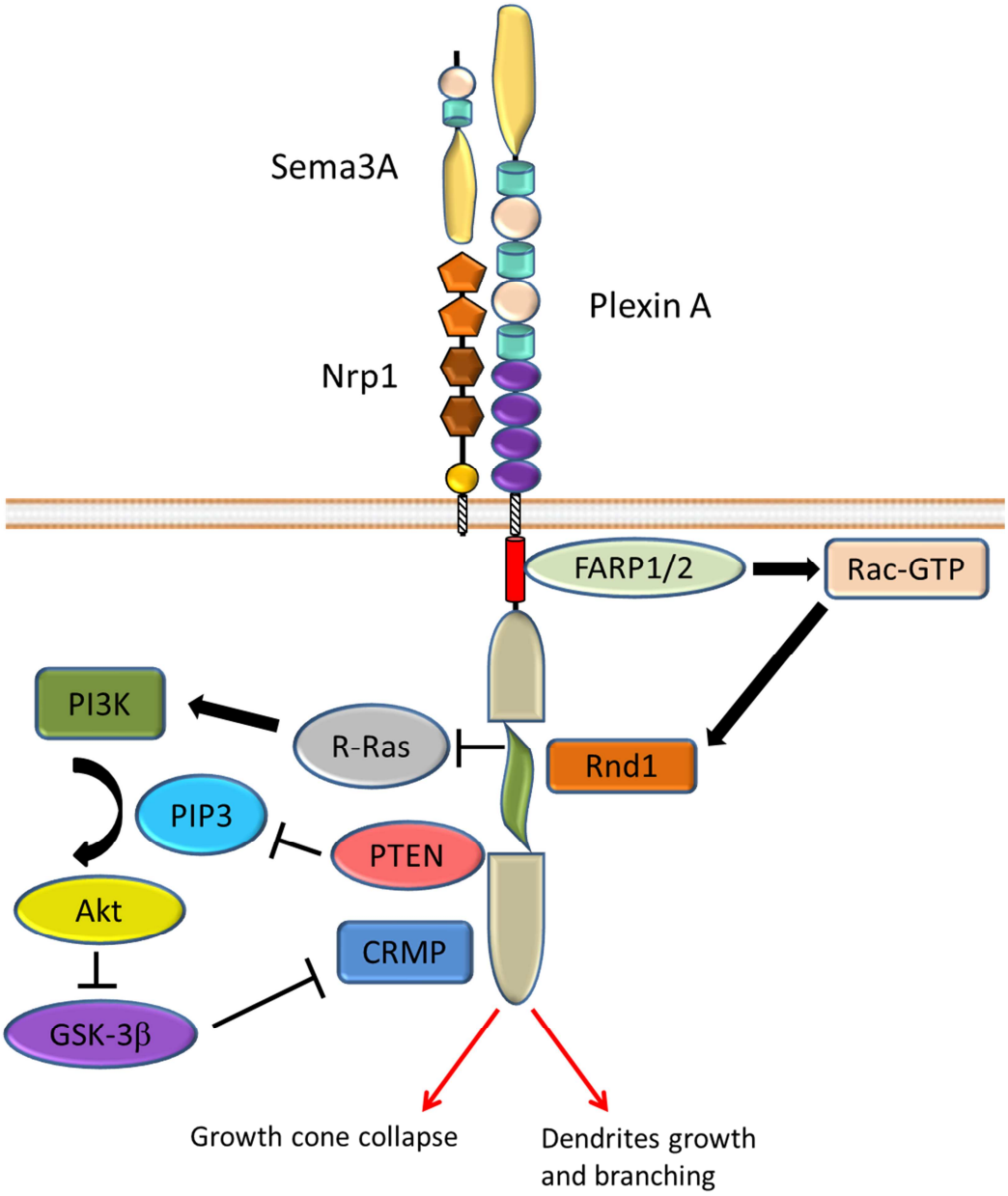

Figure 4. Illustrate signal transduction of type A Plexin

Summary of known signal transduction and effectors associate with PlexinA. (Figure modified form Tran *et al*.) (*30*)

Figure 5.

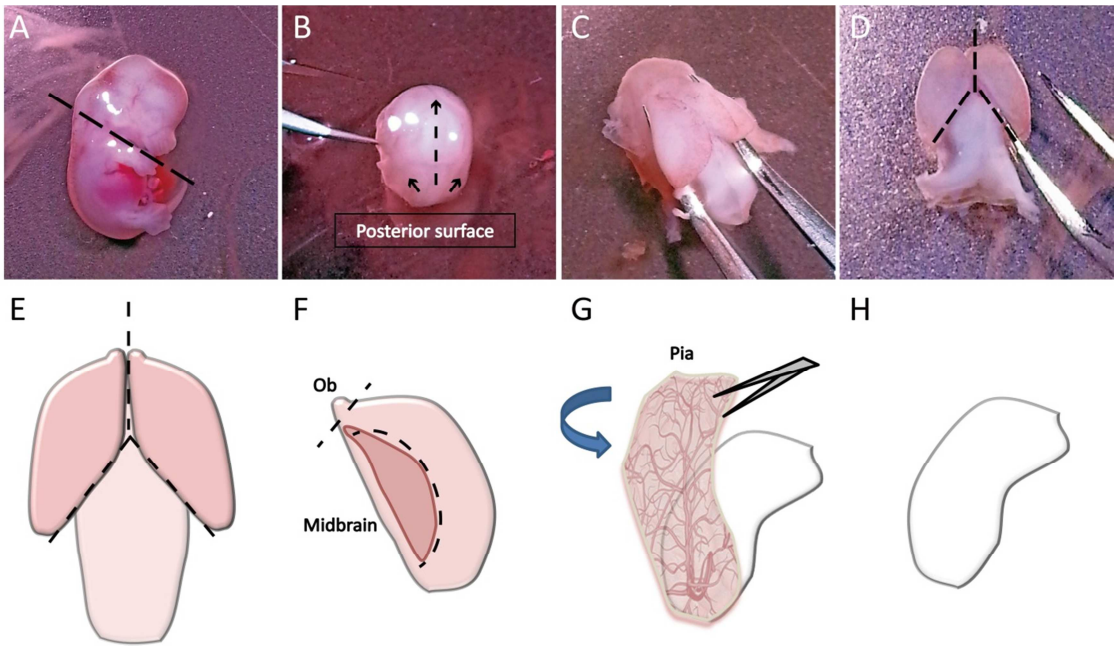

Figure 5. Illustration of dissection and isolation of cortices from the E13.5 mouse embryo

(A) Removed the head of embryo with a transverse cut (dotted lines) in a 35 mm tissue culture dish with ice-cold L-15 media. **(B)** Peeled off the skin and future skull tissues starting from the posterior end (arrows) of the head towards the anterior (dotted-line arrow). **(C)** The entire cerebral cortex and the brain stem were exposed. Using a No. 5 forceps (at a 45° angle) underneath the intact brain and brainstem to separate and remove them from the ventral side of the embryo's head. **(D-E)** Separate the cerebral hemispheres from the brainstem by making small incisions along the side of the hemisphere (dotted-lines). **(F)** Pinched off the olfactory bulb, and remove the diencephalon and future midbrain. **(G)** Rotated the hemisphere, and then use forceps peeled away the pia meningeal tissue with blood vessels. (**H)** The isolated cortices are opaquely white.

Figure 6.

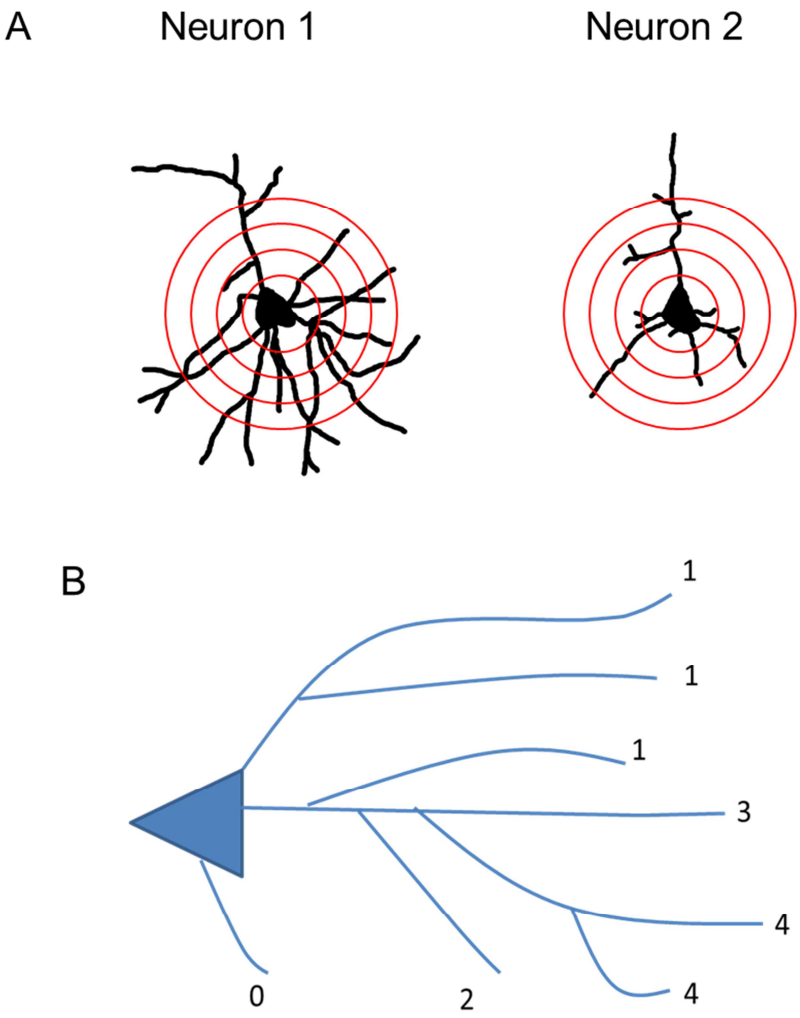

Figure 6. Schematic of Sholl analysis and DCI branch order

(A) Diagram of Sholl analysis which measure the combination of dendrite length and branch. Neuron 1 has higher intersection number represent longer dendrites and more dendrite branch than neuron 2. **(B)** Diagram illustrating branch order for DCI analysis. Each branch tip is assigned a number (0–4) that equals the number of times a primary dendrite branches to produce the branch tip.

Figure 7.

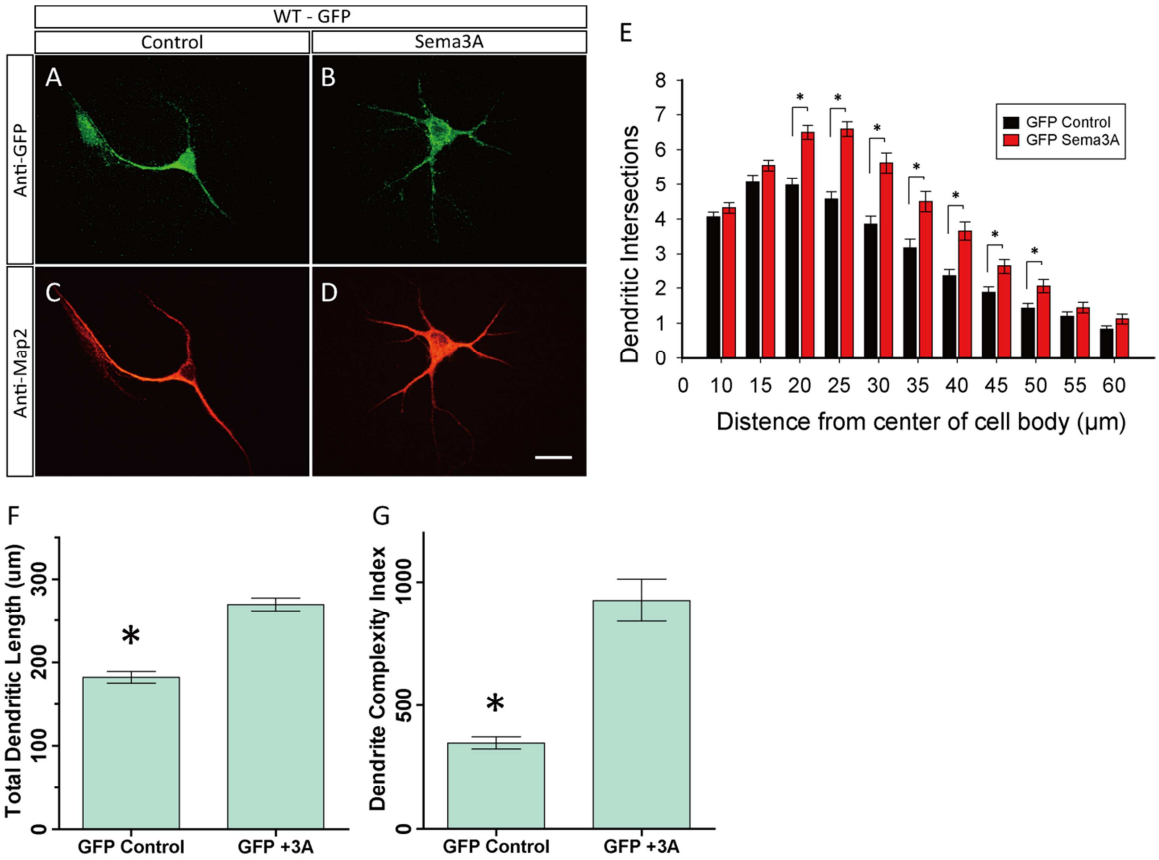

Figure 7. Illustration of dendrite measurement in three distinct analysis methods
(A-D) Representative confocal micrographs of dissociated cortical neurons from E13.5 wild type mouse embryos. Neurons were transfected with GFP DNA construct and culture for 5 DIV and stimulate with 5 nM of Sema3A proteins or control medium for additional 24 hours. Neurons were fixed and double labeled with GPF (green) and MAP2 (red). (**E)** Sholl analysis illustrates the average dendritic intersections at defined distances away from the center of the cell body. (**F, G)** Quantifications of the total dendritic length (F) and dendrite complexity index (G) are shown. Scale bar = 20µm in D for A-D. Error bars, ±S.E.M; unpaired two tails T-test was performed in E-G. Comparisons between Sema3A treatment vs. control, *P<0.01 in (E), *P<0.001 in (F, G).

Figure 8.

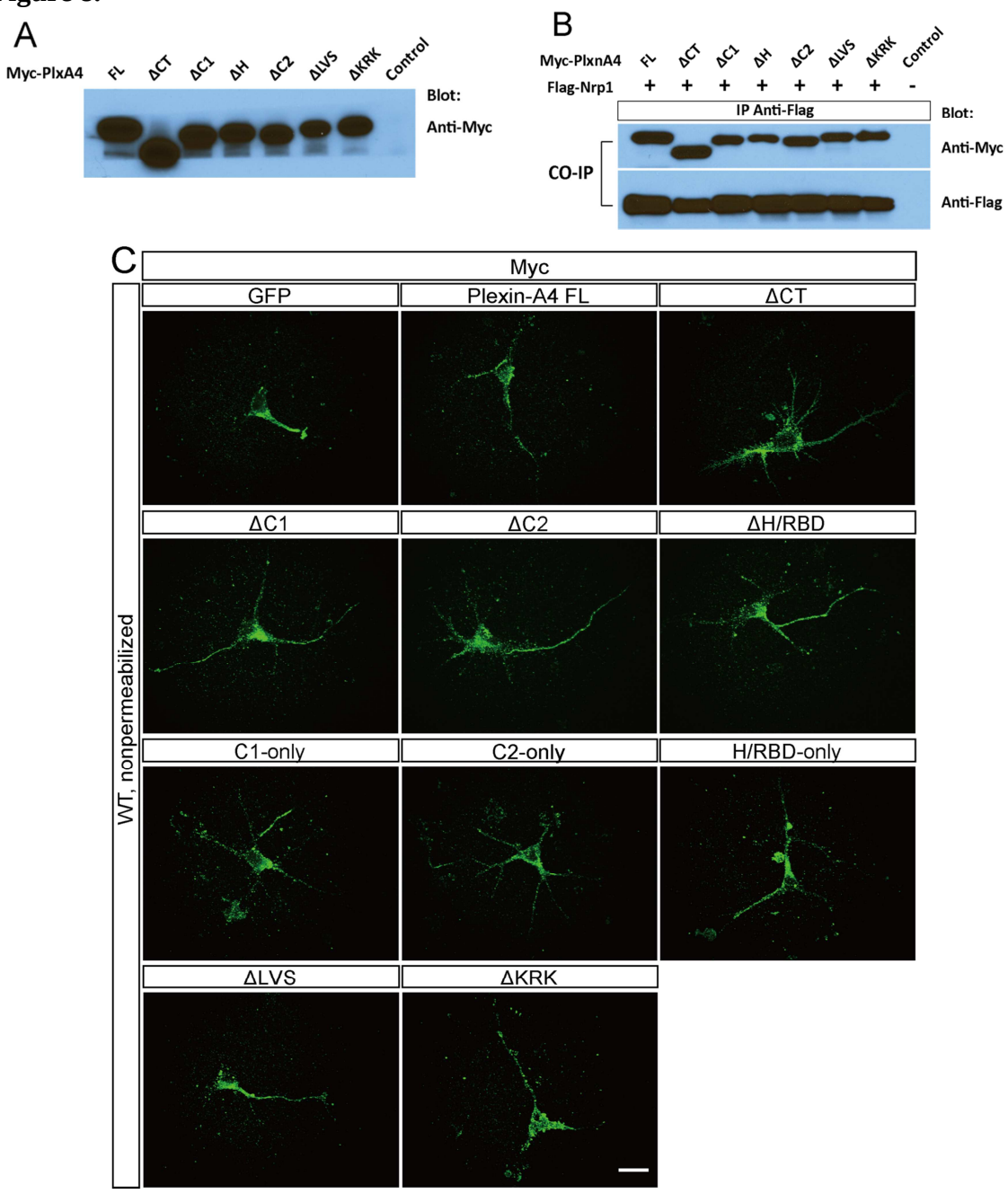

Figure 8. Validation of PlxnA4 mutants constructs

PlxnA4 mutants were transfected to HEK293 cells culture for 48 hours (A, B) or transfected to mouse cortical neurons culture 6 days (C) to test out the protein expression. **(A)** Western blot of PlxnA4 mutants with anti-Myc antibody. **(B)** CO-IP for PlxnA4 mutants and Nrp1. Protein were pull down by anti-flag and blotting with anti-Myc and anti-flag antibodies. **(C)** PlxnA4 mutants expressed on cortical neuron surface. Neurons were fixed and stained with Myc antibody (green) without permeabilization.

Figure 9.

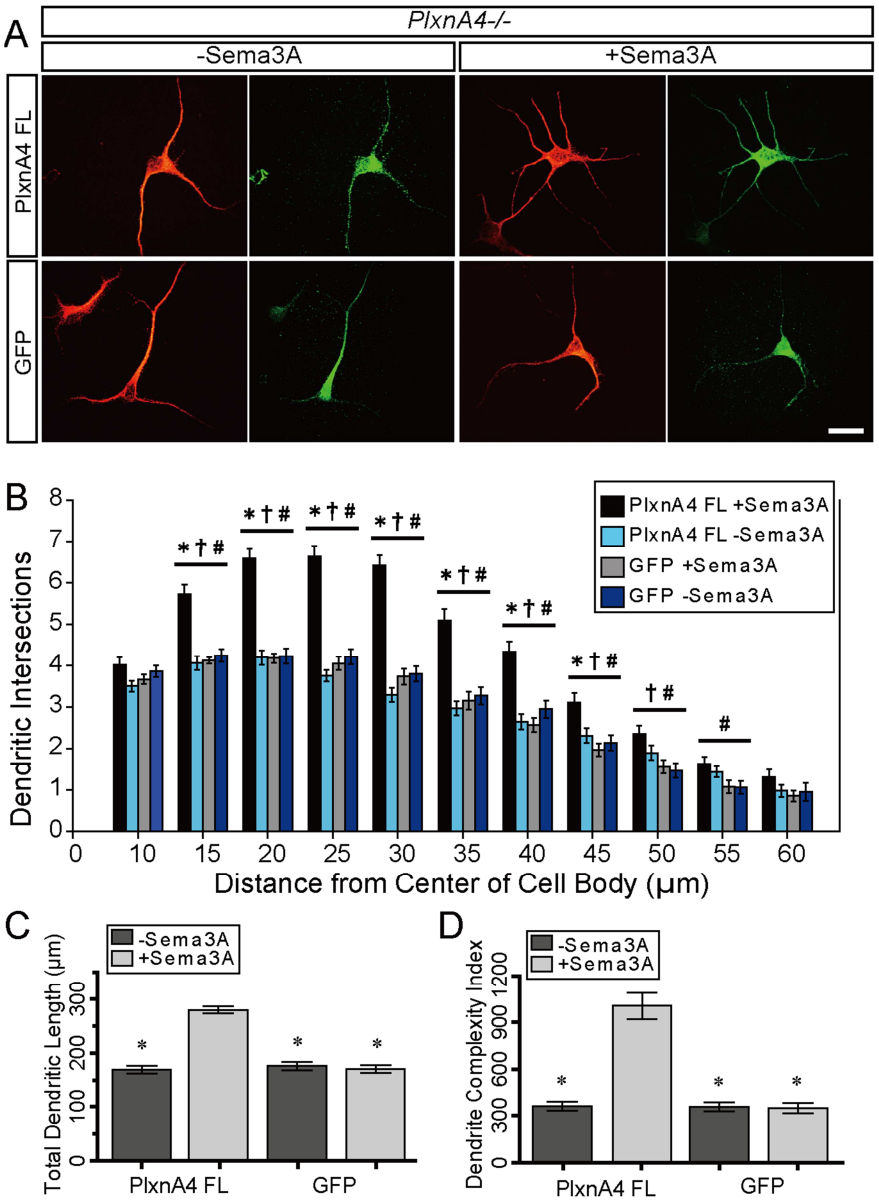

Figure 9. PlxnA4 KO neurons dendritic growth and branching defects can be rescued by PlxnA4 and Sema3A in culture

(A) E13.5 PlxnA4 KO cortical neuron were dissected and transfected with Myc-tagged PlxnA4 FL or GFP and treated with 5 nM AP (−Sema3A) or AP-tagged Sema3A (+Sema3A) for 24 hours and stained for Myc (green) and MAP2 (red). (B to D) Quantification of dendritic growth and branching: Sholl analysis **(B)**, total dendritic length **(C)**, and DCI **(D)**. Scale bar, 20 μm.Data are means ± SEM from three to four independent cultures of each construct, with 40 neurons each were analyzed. Compared with PlxnA4 FL + Sema3A: in (B), $P < 0.01$ for PlxnA4 FL – Sema3A (*), GFP + Sema3A (†), and GFP – Sema3A (#); in (C) and (D), $*P < 0.001$; one-way analysis of variance (ANOVA) followed by post hoc Tukey test.

Figure 10-1.

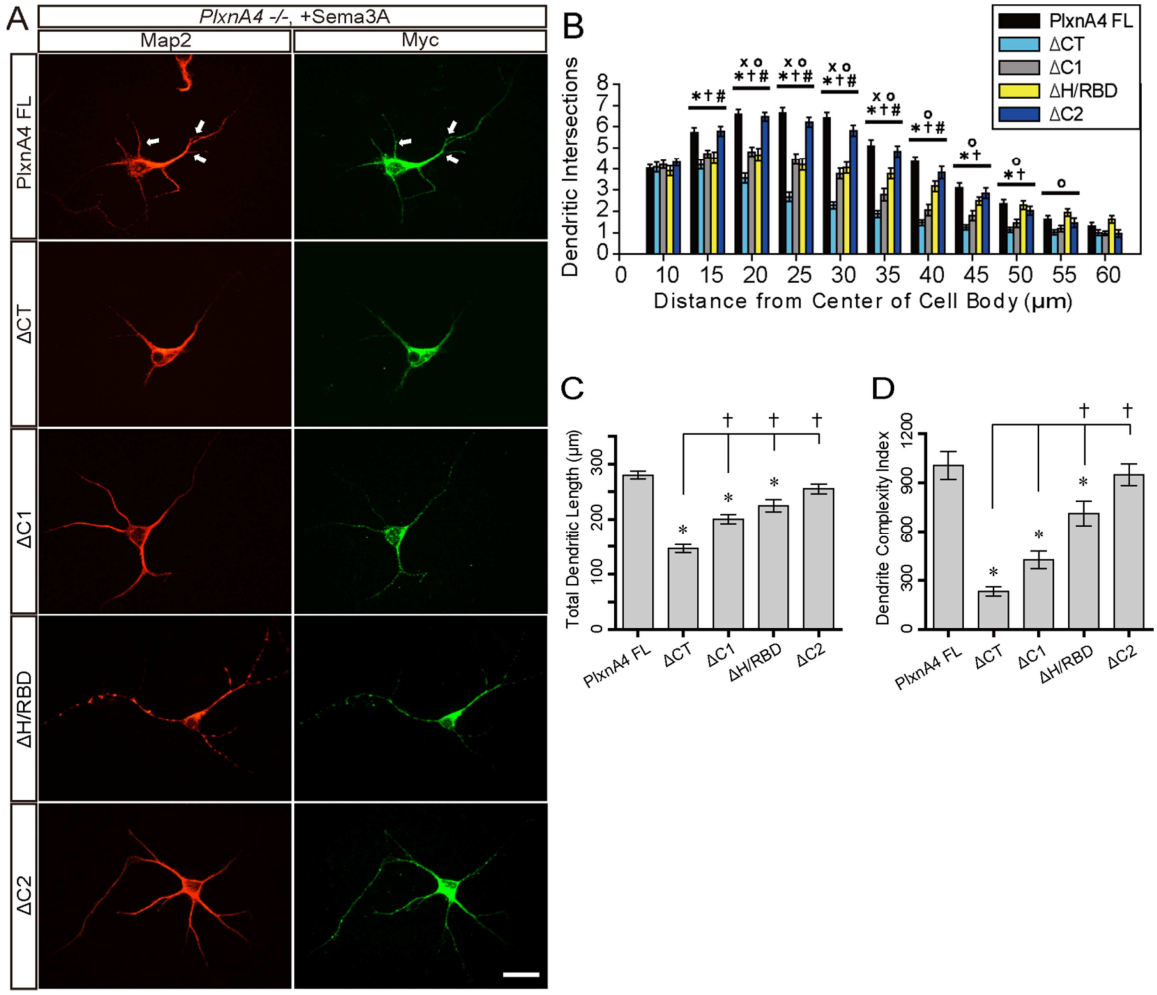

Figure 10-1. Distinct PlxnA4 cytoplasmic domains regulate dendritic morphogenesis of PlxnA4 KO cortical neurons

(A) Representative confocal figures of primary cortical neurons from E13.5 embryos transfected with Myc-tagged PlxnA4 FL or mutants. Overexpression of PlxnA4 was detected in soma and dendrites (white arrows) as seen with MAP2 (red) and Myc (green) labeling. **(B to D)** Quantification of dendritic growth and branching: Sholl analysis (B), total dendritic length (C) and DCI (D). Scale bar, 20μm in (A). For every construct, N = 3 to 4 independent cultures, 35 neurons were analyzed. Data are means ± SEM. In (B) $P<0.01$ for all comparisons between PlxnA4 FL and ΔCT (*), ΔC1 (†), ΔH/RBD (#); $P<0.01$ for ΔCT compared with ΔC1 (o), ΔH/RBD (x). In (C), (D) *$P < 0.001$, versus PlxnA4 FL; †$P < 0.05$, versus ΔCT; one-way ANOVA followed by post hoc Tukey test.

Figure 10-2.

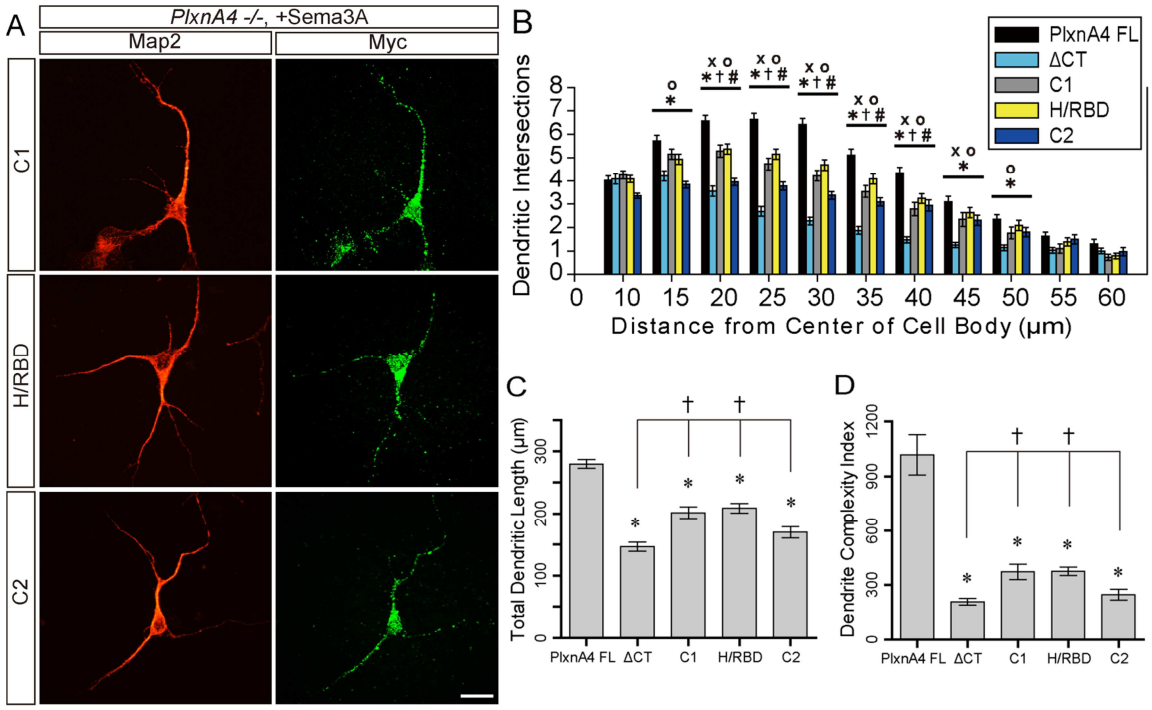

Figure 10-2. Distinct PlxnA4 cytoplasmic domains regulate dendritic morphogenesis of PlxnA4 KO cortical neurons

(A) Representative confocal figures of primary cortical neurons from E13.5 embryos transfected with Myc-tagged PlxnA4 FL or mutants. Overexpression of PlxnA4 was detected in soma and dendrites (white arrows) as seen with MAP2 (red) and Myc (green) labeling. **(B to D)** Quantification of dendritic growth and branching: Sholl analysis (B), total dendritic length (C) and DCI (D). Scale bar, 20μm in (A). For every construct, N = 3 to 4 independent cultures, 35 neurons were analyzed. Data are means ± SEM. In (B) $P<0.01$ for all comparisons between PlxnA4 FL and ΔCT (*), C1 only (†), H/RBD only (#); $P<0.01$ for ΔCT compared with C1 only (o), H/RBD only (x). In (C), (D) *$P < 0.001$, versus PlxnA4 FL; †$P < 0.05$, versus ΔCT; one-way ANOVA followed by post hoc Tukey test.

Figure 11.

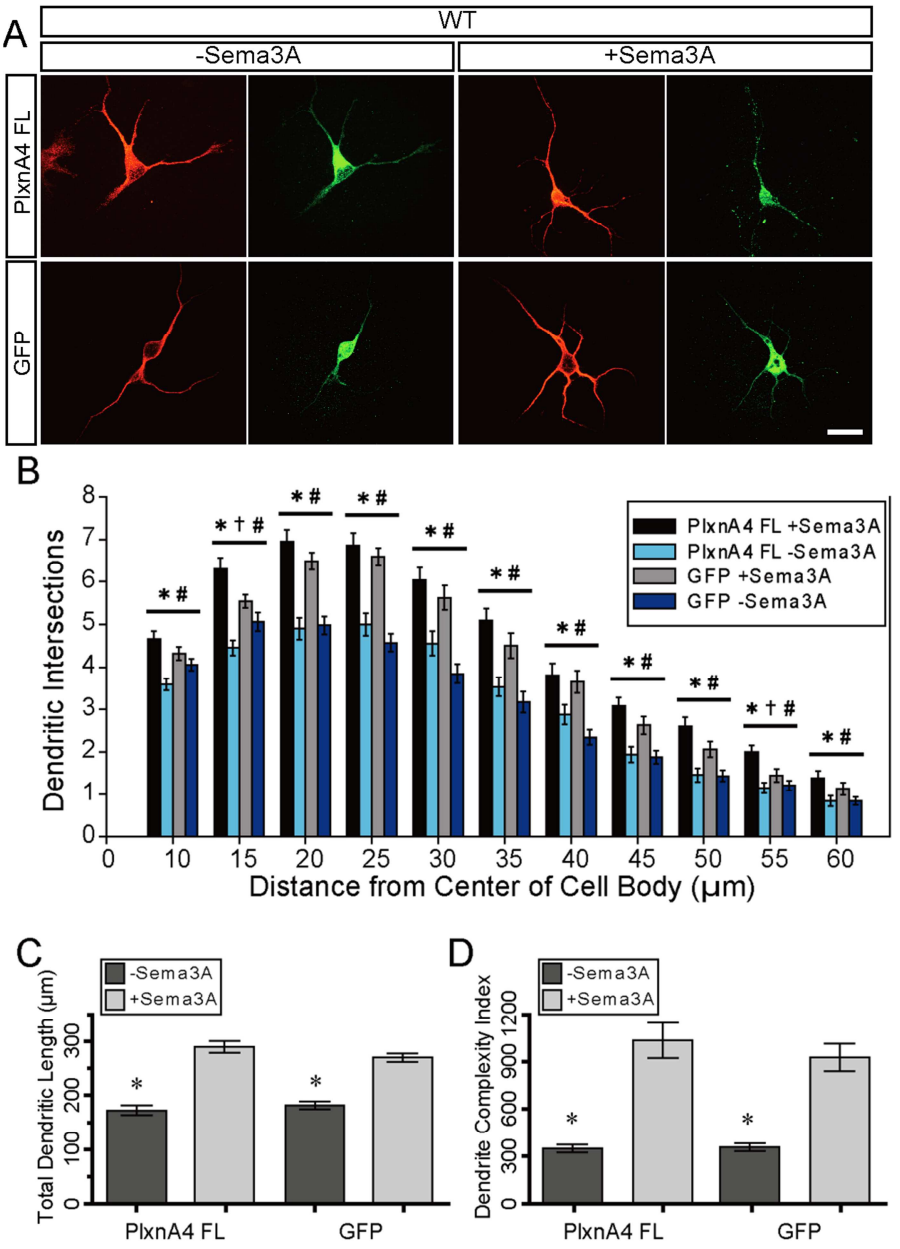

Figure 11. No gain-of-function in PlxnA4 overexpressed WT neuron

(A) Representative images of WT E13.5 mouse cortical neurons transfected with Myc-PlxnA4 FL or GFP. Neuron stimulated with AP-Sema3A (Sema3A) or with AP-alone control (-Sema3A) and stained for Myc (green) and MAP2 (red). **(B)** Sholl analysis of average dendritic intersections. **(C)** Quantification of total dendritic length and **(D)** DCI. Scale bar, 20μm. Data are means ± SEM from four independent cultures with 50 neurons each were analyzed. Compared with PlxnA4 FL + Sema3A: in (B), $P < 0.01$ for PlxnA4 FL – Sema3A (*), GFP + Sema3A (†), and GFP – Sema3A (#); in (C) and (D), *$P < 0.001$; one-way ANOVA followed by post hoc Tukey test.

Figure 12.

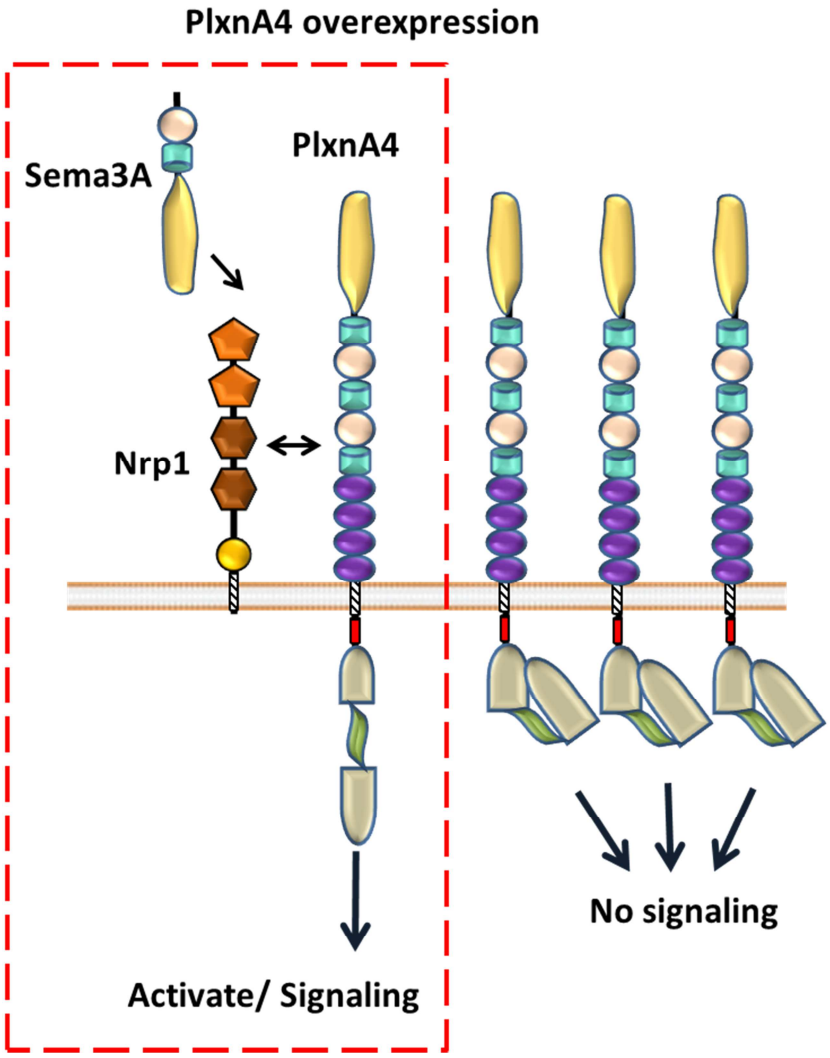

Figure 12. Schematic diagram of activate receptor complex in PlxnA4 overexpressed neurons

Schematic diagram illustrating limited level of PlxnA4 can forming activate receptor complex due to the number of endogenous Neuropilin-1 (Nrp1). Overexpressed PlxnA4 without binding Nrp1 won't be able to start signaling.

Figure 13-1.

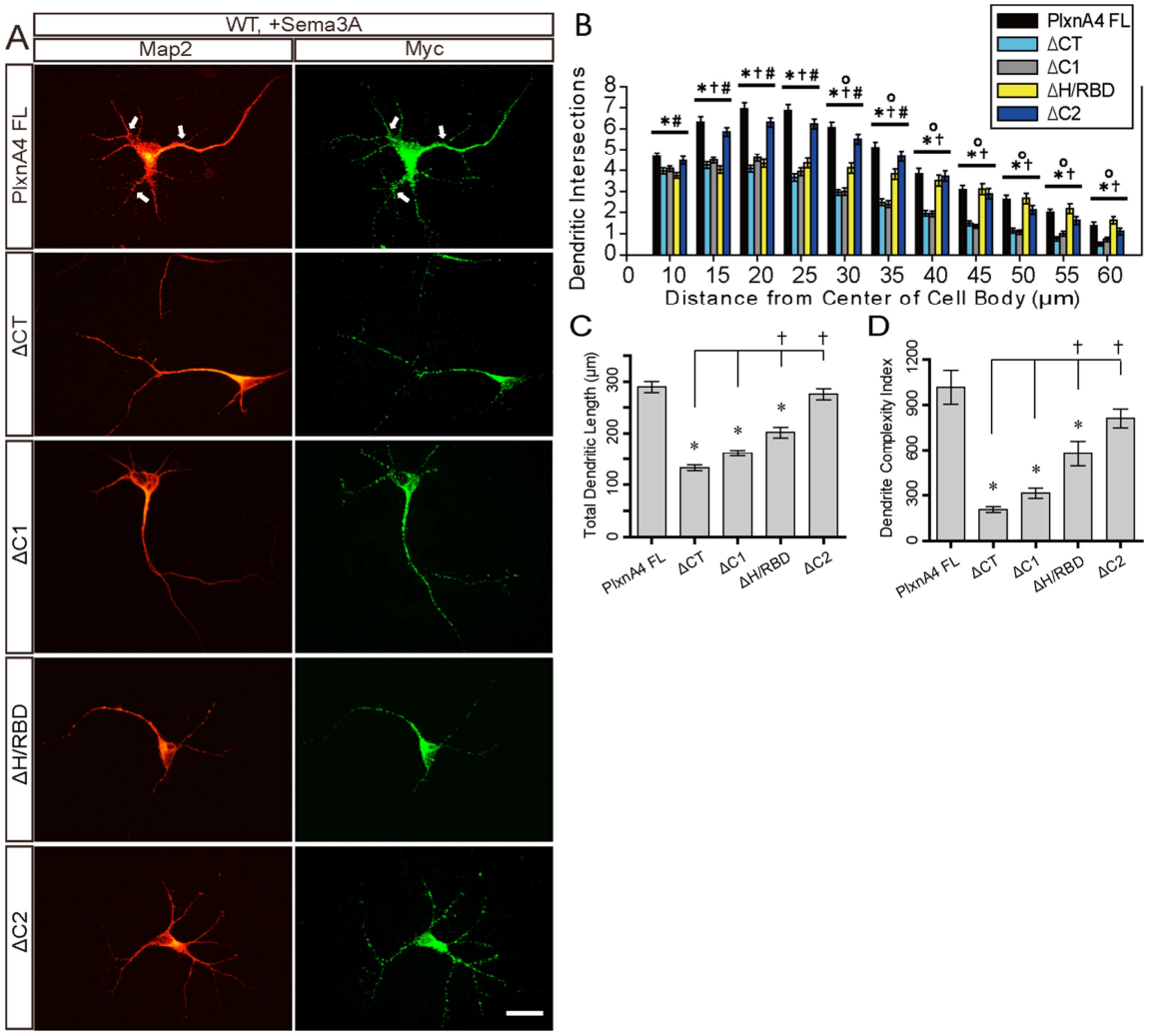

Figure 13-1. PlxnA4 cytoplasmic domains regulate wild-type cortical neuron dendrite arborization

(A) Myc (green) and MAP2 (red) double staining in cortical neurons dissociated from E13.5 embryos, transfected with Myc-tagged PlxnA4 variants, and treated with 5 nM Sema3A for 24 hours. White arrows: PlxnA4 expression in soma and dendrites. **(B to D)** Quantification of dendritic growth and branching analysis: sholl analysis (B), total dendritic length (C) and DCI (D). Scale bar, 20μm in (A). For every construct, N = 3 to 4 independent cultures, least 50 neurons were analyzed for each mutant. Data are means ± SEM. In (B) $P<0.01$ for all comparisons between PlxnA4 FL and ΔCT (*), ΔC1 (†), ΔH/RBD (#); $P<0.01$ for ΔCT compared with ΔC1 (o), ΔH/RBD (x). In (C), (D) *$P < 0.001$, versus PlxnA4 FL; †$P < 0.05$, versus ΔCT; one-way ANOVA followed by post hoc Tukey test.

Figure 13-2.

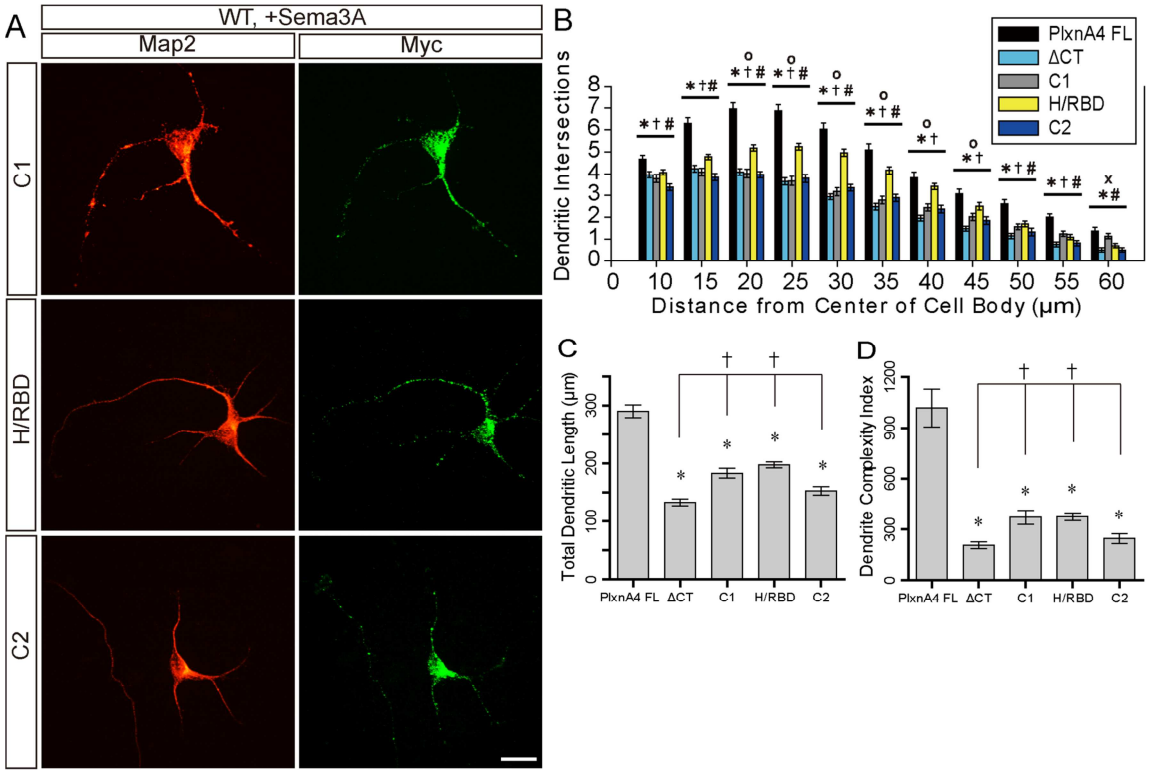

Figure 13-2. PlxnA4 cytoplasmic domains regulate wild-type cortical neuron dendrite arborization

(A) Myc (green) and MAP2 (red) double staining in cortical neurons dissociated from E13.5 embryos, transfected with Myc-tagged PlxnA4 variants, and treated with 5 nM Sema3A for 24 hours. **(B to D)** Quantification of dendritic growth and branching analysis: sholl analysis (B), total dendritic length (C) and DCI (D). Scale bar, 20μm in (A). For every construct, N = 3 to 4 independent cultures, least 50 neurons were analyzed for each mutant. Data are means ± SEM. In (B) $P<0.01$ for all comparisons between PlxnA4 FL and ΔCT (*), C1 only (†), H/RBD only (#); $P<0.01$ for ΔCT compared with C1 only (o), H/RBD only (x). In (C), (D) *$P < 0.001$, versus PlxnA4 FL; †$P < 0.05$, versus ΔCT; one-way ANOVA followed by post hoc Tukey test.

Figure 14.

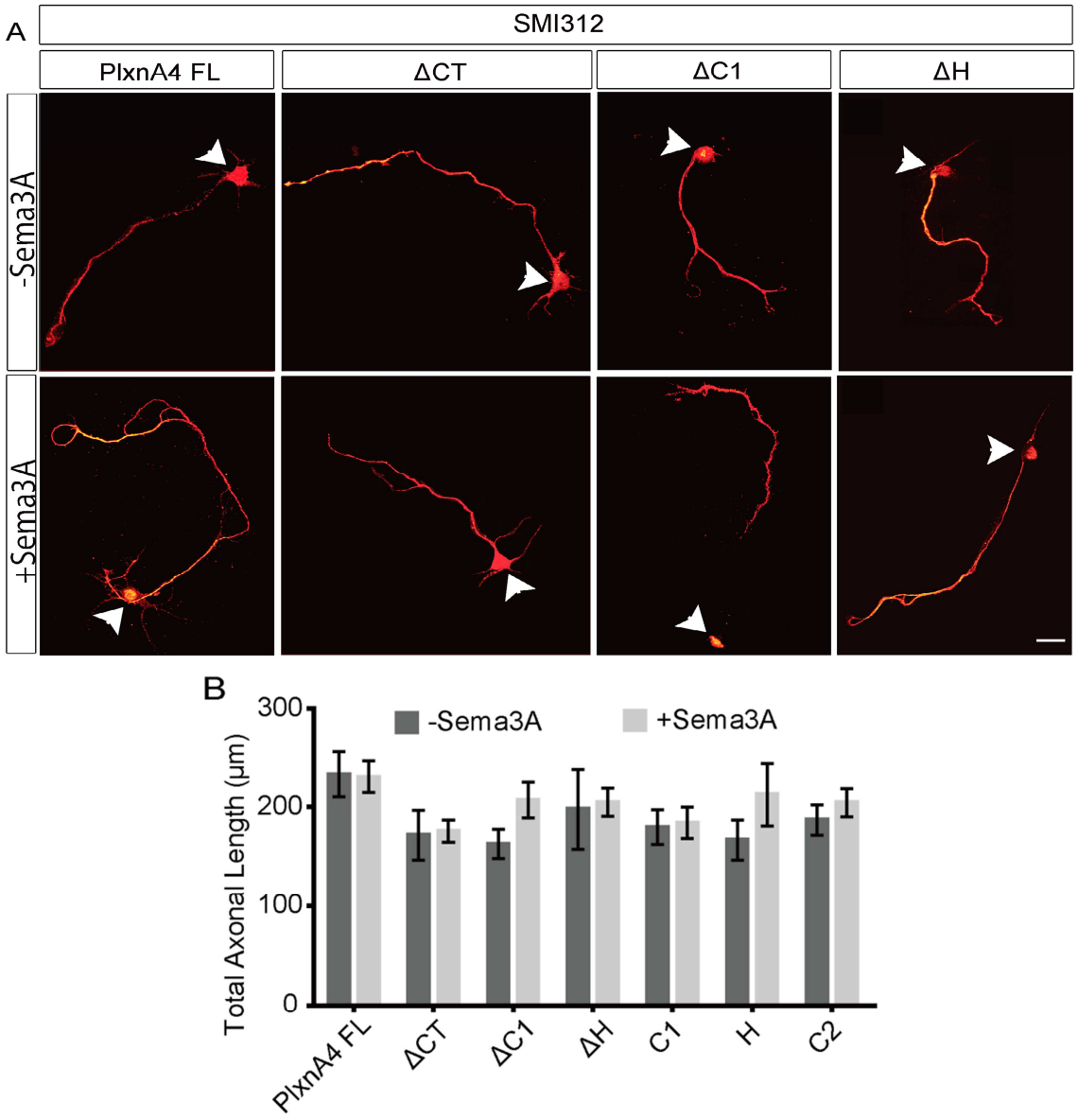

Figure 14. Axonal length does not affected by Sema3A/PlxnA4 mutant signaling in wild-type cortical neurons

(A) Representative confocal micrographs illustrate WT E13.5 primary cortical neurons transfected with PlxnA4 FL, ΔCT, ΔC1, or ΔH. These neurons were treat with 5nm AP-Sema3A (+Sema3A) or AP-alone (-Sema3A) and stained for SMI312 (pan-axonal neurofilament marker). Scale bar = 20 µm in A. Arrowheads, soma. **(B)** Quantification of Axonal length with Sema3A treatment (1.5 hour). For every construct, n=3 independent cultures with a total of 15-18 neurons were analyzed. Data are means ± SEM; one-way ANOVA was performed followed by post-hoc Tukey test.

Figure 15.

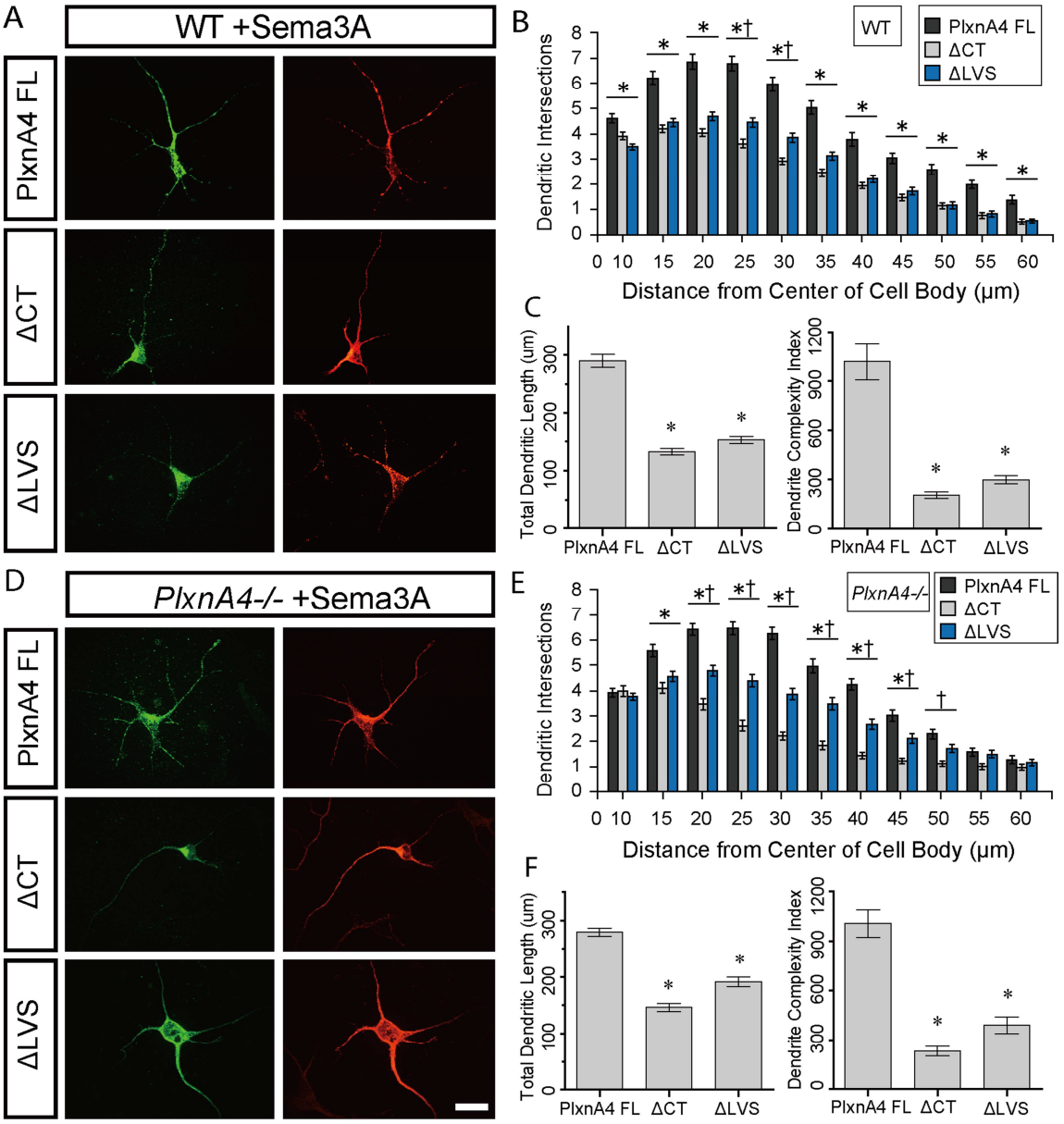

Figure 15. The LVS motif is required for Sema3A/PlxnA4 mediated dendritic arbor PlxnA4 FL, ΔCT or ΔLVS were transfected into WT or PlxnA4 KO cortical neurons culture for 6 DIV and treat with 5nm Sema3A. Neurons then fixed and stained with Myc (green) and MAP2 (red). **(A, D)** Representative confocal pictures of PlxnA4 transfected neurons, (A) WT, (D) PlxnA4 KO neurons. **(B, E)** Sholl analysis quantified the number of dendritic intersections. **(C, F)** Quantification of total dendritic length and DCI in WT and KO neurons. Scale bar = 20 μm in D. Data are means ± SEM from four to five independent cultures in which a total 35 neurons were analyzed per PlxnA4 variant. In (B) and (E), *P < 0.01 for PlxnA4 FL versus ΔLVS, †P < 0.01 for ΔCT versus ΔLVS. In (C) and (F), *P < 0.001 versus PlxnA4 FL; one-way ANOVA followed by post hoc Tukey test.

Figure 16.

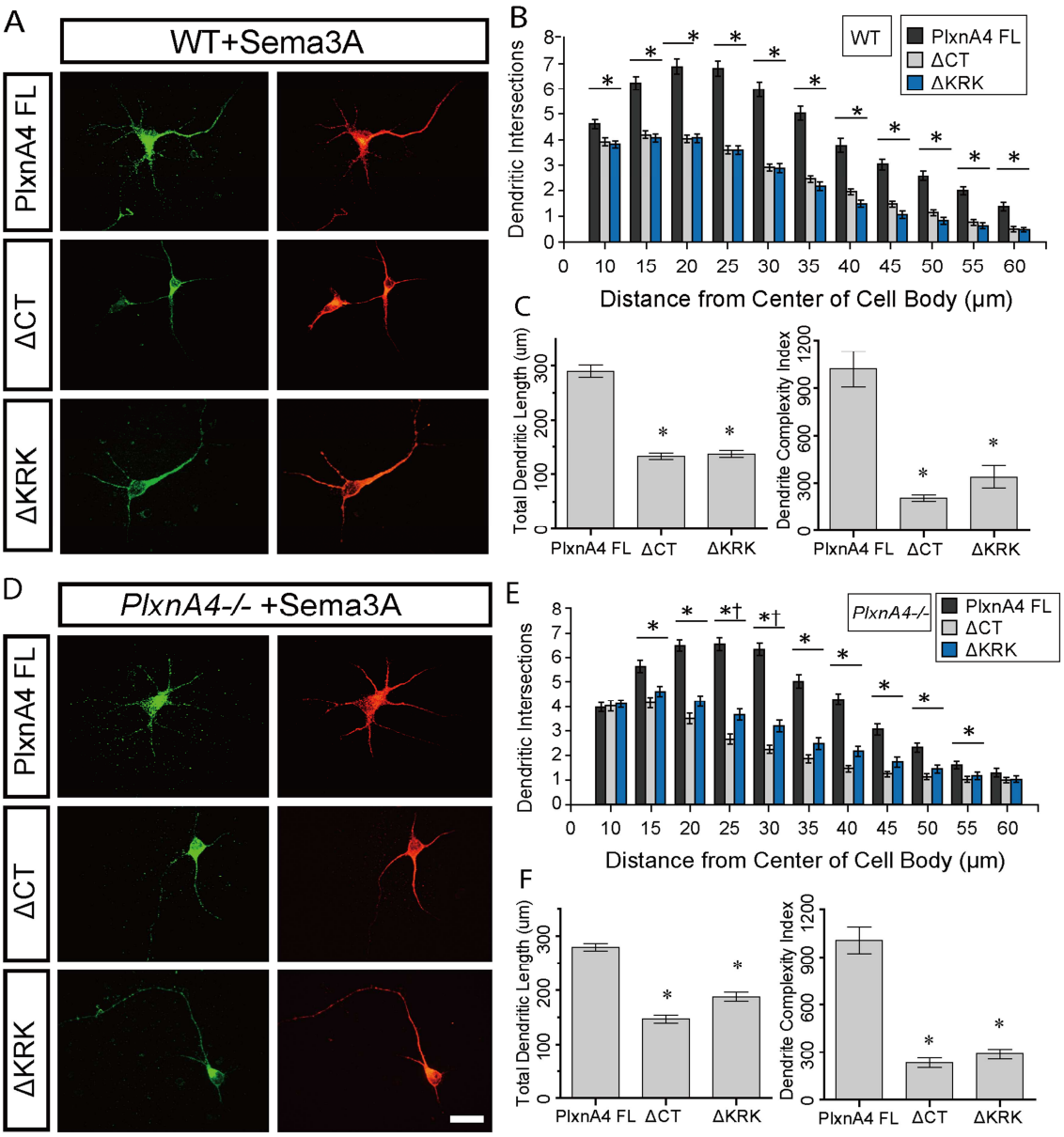

Figure 16. The KRK motif is necessary for Sema3A/PlxnA4 mediate dendrite promoting

Dissociated WT or PlxnA4 KO neurons were transfected with PlxnA4 FL, ΔCT or ΔKRK and culture 6DIV. Neurons treated with 5nm Sema3A and stained with Myc (green) and MAP2 (red). **(A, D)** Confocal pictures of PlxnA4 transfected neurons, (A) WT, (D) PlxnA4 KO neurons. (B, C, E, F) Quantification of WT or PlxnA4 KO neurons' dendritic growth and branching: sholl analysis **(B, E)**, total dendritic length and DCI **(C, F)**. Scale bar = 20 μm in (D). Data are means ± SEM from four independent cultures in which at least 35 neurons were analyzed for each PlxnA4 mutant. In (B) and (E), *P < 0.01 for PlxnA4 FL versus ΔLVS, †P < 0.01 for ΔCT versus ΔLVS. In (C) and (F), *P < 0.001 versus PlxnA4 FL; one-way ANOVA followed by post hoc Tukey test.

Figure 17.

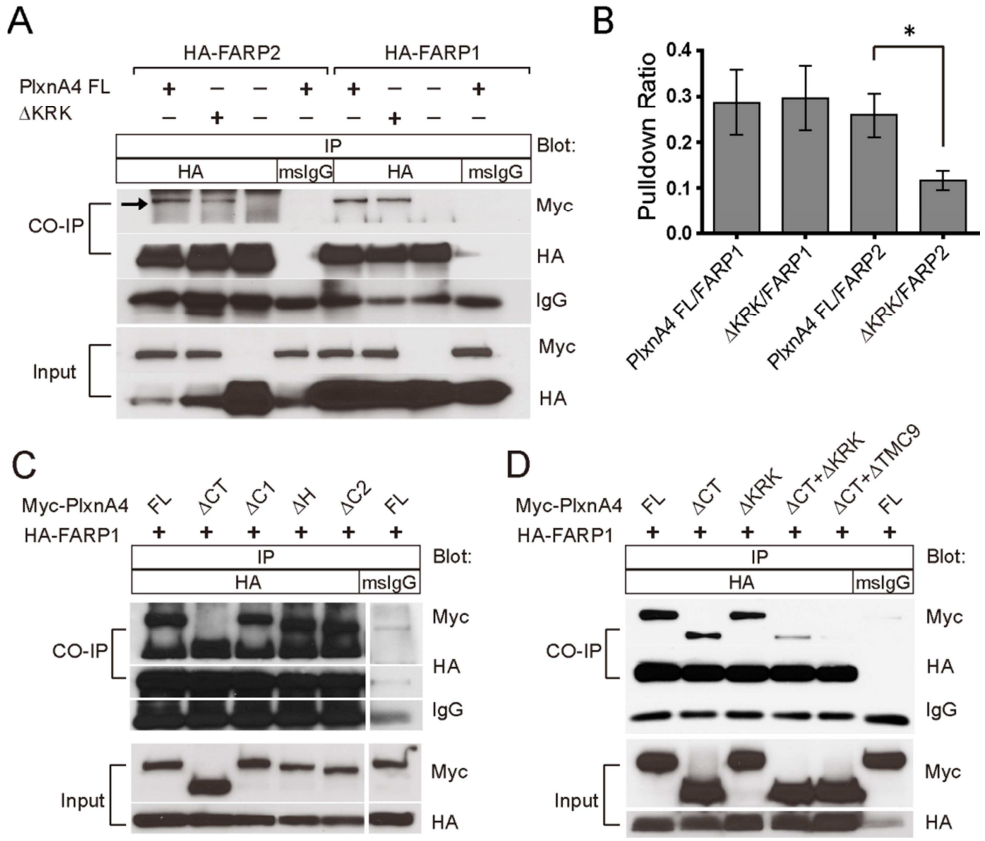

Figure 17. FARP1 and FARP2 interact with PlxnA4 KRK and additional juxtamembrane region

(A) CO-IP between Myc-tagged PlxnA4 FL or ΔKRK and HA-tagged FARP1 or FARP2 in HEK293 cells. Arrow in the blot indicates myc-Plexins. IP using anti-HA antibody for pull down and mouse IgG for control. **(B)** Quantification of pull down ratio; Error bars, ±SEM *P<0.05, two-tailed Student's T test used to analyze the ratio (n=4). **(C)** Additional CO-IP between Myc-tagged PlxnA4 constructs with HA-tagged FARP1 in HEK293 cells. **(D)** Western blot of CO-IP between new PlxnA4 constructs and HA-FARP1 in HEK293 cells. Blot is representative of three experiments.

Figure 18.

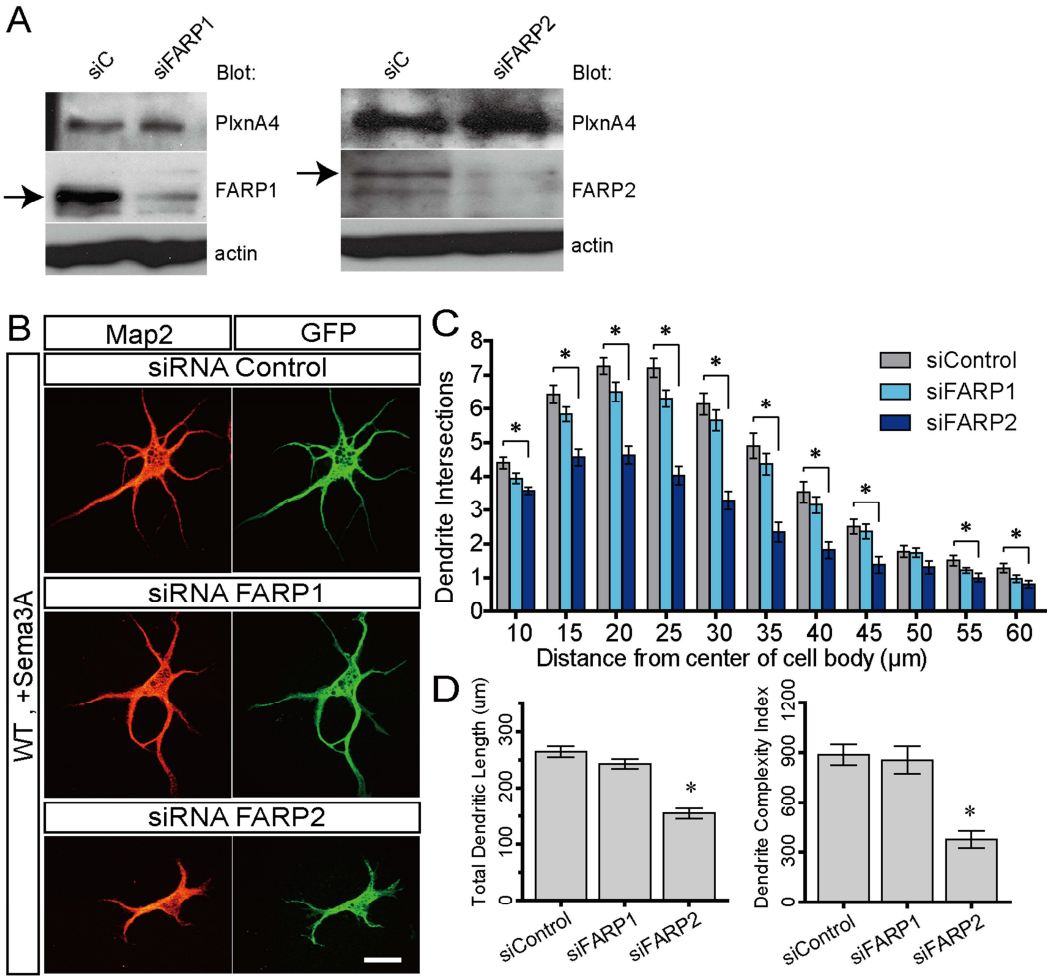

Figure 18. FARP1 and FARP2 siRNA knockdown: FARP2 is required for cortical neuron dendrite arborization

(A) Validation of siRNA knockdown. Western blot for PlxnA4, FARP1, and FARP2 abundance in whole cell lysates of cortical neurons from WT E13.5 mouse embryos transfected with either a control siRNA, siRNA against FARP1, or siRNA against FARP2.Arrow indicate the FARP proteins. Small interfering RNAs effectively reduce expression of FARP proteins. **(B)** Representative images for siRNA and GFP co-transfected WT cortical neurons. All Neurons were double labeled with anti-GFP (green) and anti-Map2 (red). FARP2 Knockdown neurons were showing much less dendrites while control and FARP1 knowckdown have no significant effects on the dendrites. **(C)** Sholl analysis of dendrite arbors **(D)** Quantification of total dendritic length and DCI for control and knockdown neurons. Only the FARP2 knockdown neurons showed the significant shorter in total dendritic length and less complexity in DCI. Three independent cultures and 35 neurons for each condition were analyzed. Error bars, ±S.E.M; one way ANOVA, and post-hoc Tukey test. In (C),*p<0.05; in (D), ***p<0.001; Scale bar = 20µm.

Figure 19.

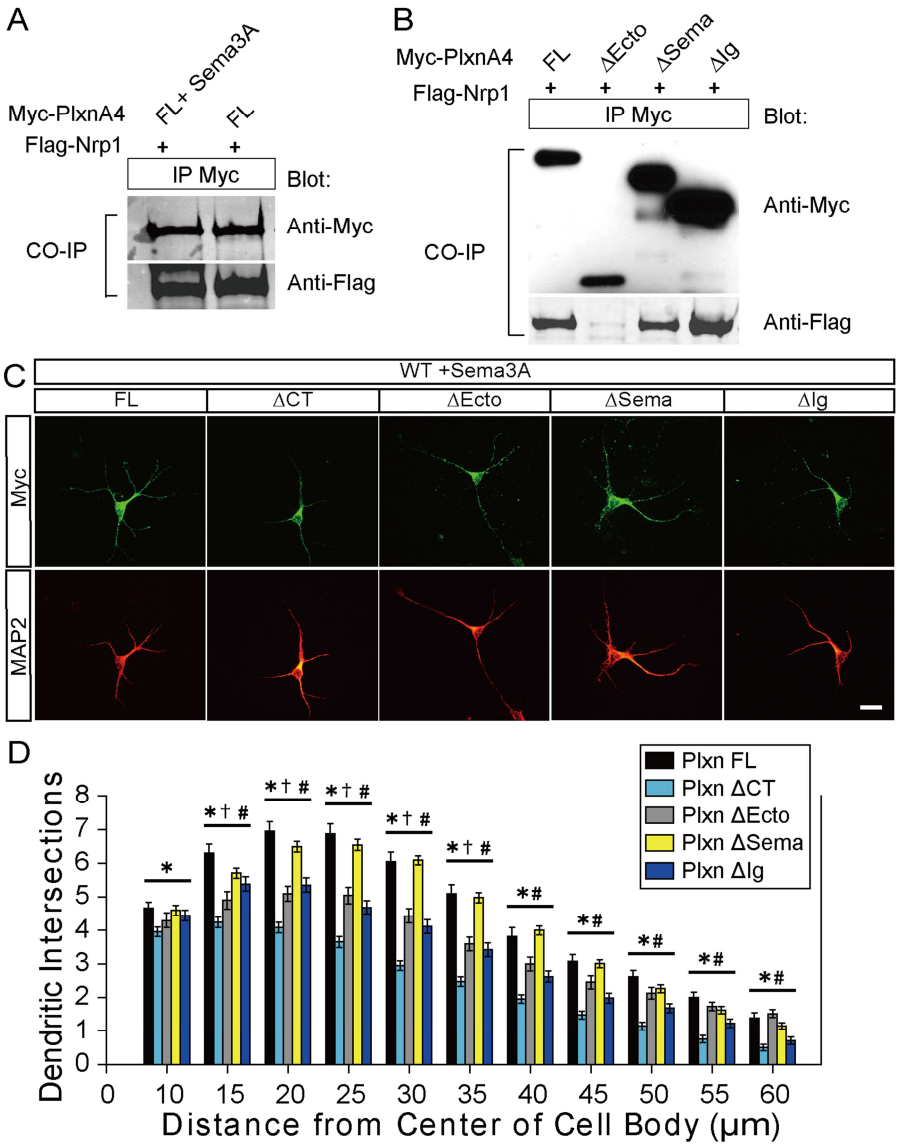

Figure 19. PlxnA4 extracellular mutants change Nrp1 binding and alter cortical neuron dendritic arbor

(A, B) Flag-Nrp1 and Myc-PlxnA4 construct were co-transfect to HEK293 cells. After 48 hours, cells were lysed and IP using anti-Myc antibody. In (A), cells treated with 5nm Sema3A or AP-along for 6 hours before lysed. No different were found. In (B), no Sema3A were treated. No interaction between Nrp1 and PlxnA4 ΔEcto. **(C)** Representative images of WT E13.5 mouse cortical neurons transfected with Myc-PlxnA4 FL or ecto mutants. Neuron stimulated with Sema3A and stained for Myc (green) and MAP2 (red). **(D)** Quantification of dendritic intersections in Sholl analysis. Scale bar, 20μm. For every construct, n = 3 to 4 independent cultures, ~50 neurons were analyzed. Data are means ± SEM. In (D), P<0.01 for all comparisons between PlxnA4 FL and ΔCT (*), ΔEcto (†), ΔIg (#); one-way ANOVA followed by post hoc Tukey test.

Figure 20.

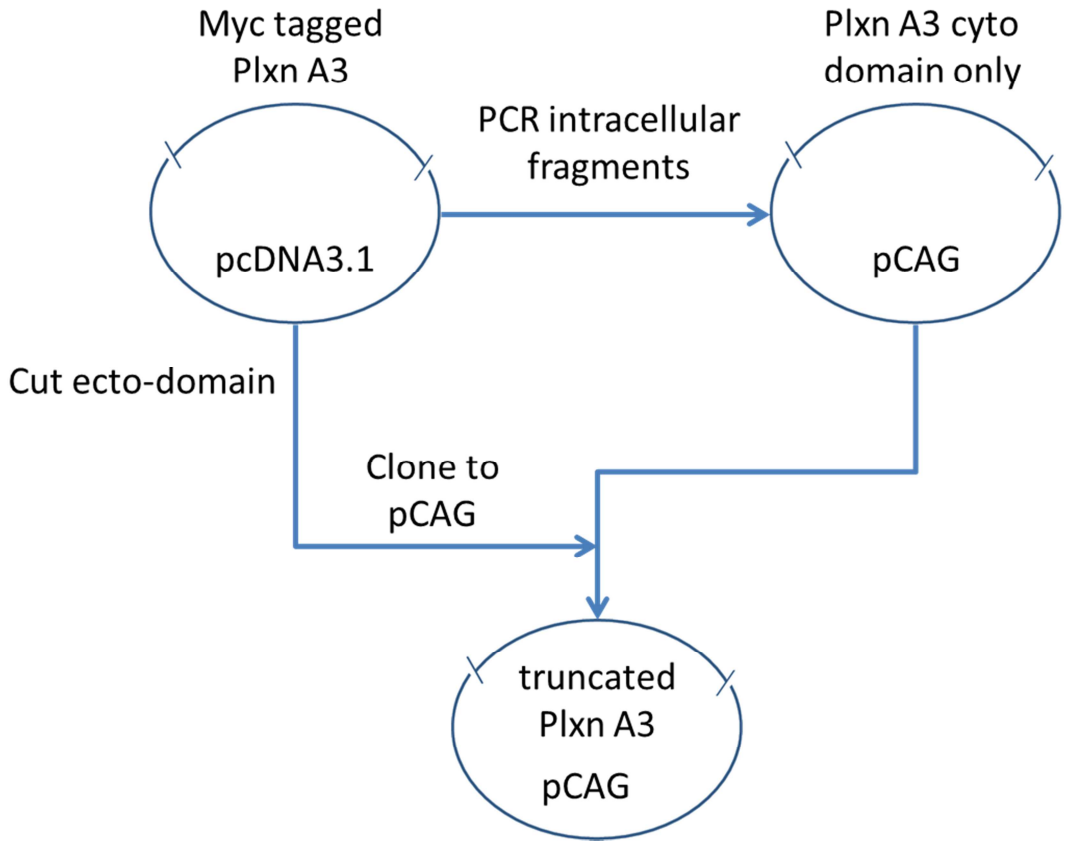

Figure 20. Schematic view of cloning strategy

Diagram illustrates the strategy of making the new Myc-tagged PlxnA3 constructs from Myc-PlxnA3 FL.

Figure 21.

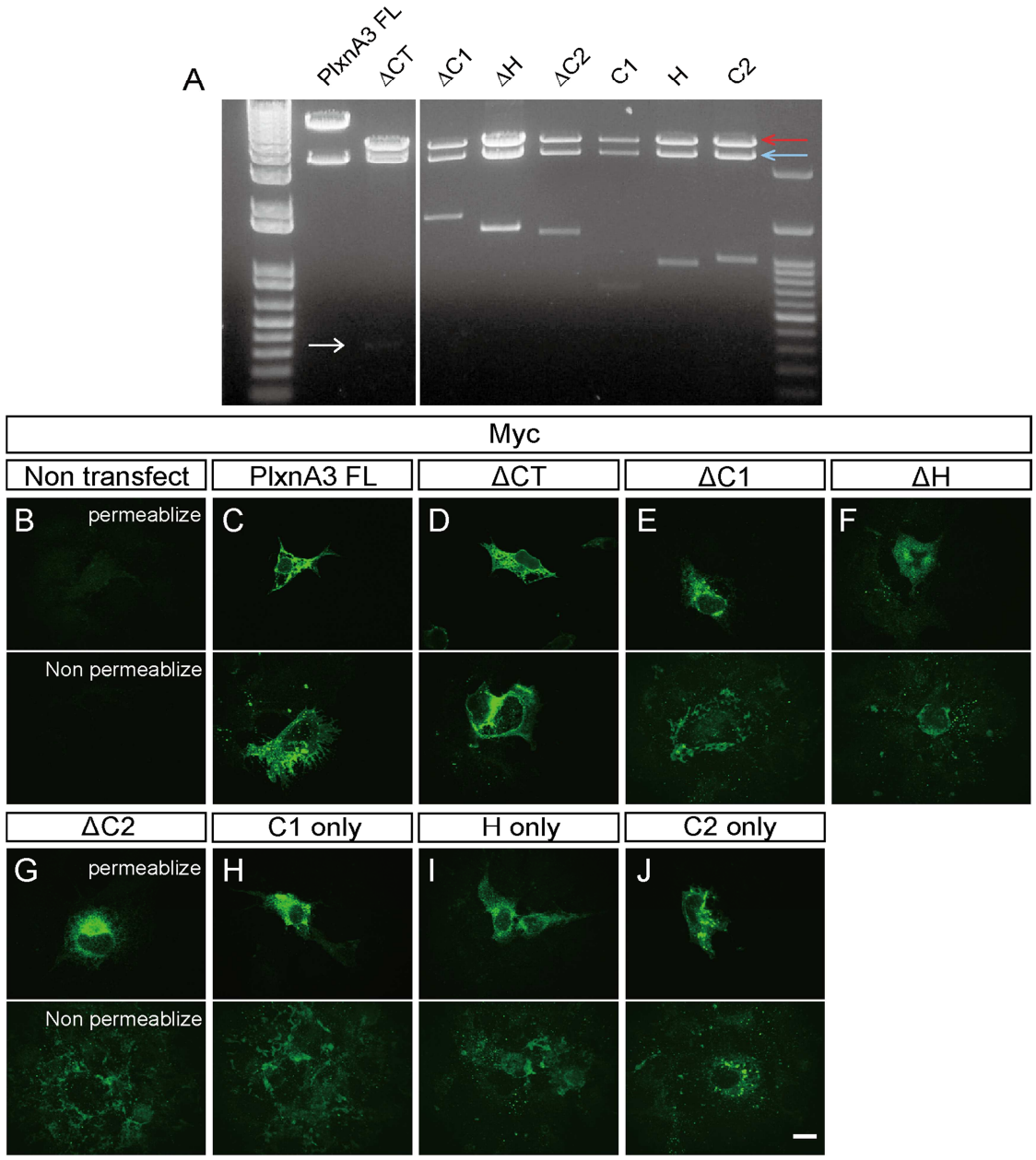

Figure 21. Validation of PlxnA3 constructs

(A) New PlxnA3 constructs restriction enzyme double digested using NotI/NheI. Red arrow: backbone (pCAG 4.8Kb); Blue arrow: ecto domain (3.7Kb). White arrow: ΔCT (303bp). Other construct's cyto-domain: ΔC1 (1587bp), ΔH (1353bp), ΔC2 (1293bp), C1 only (678bp), H only (915bp), A3 C2 only (975bp) **(B-J)** PlxnA3 mutants transfected to COS7 cells for 48 hours and stained with anti-Myc antibody either with Triton-X or no Triton-X. Scale bar, 20μm.

Figure 22.

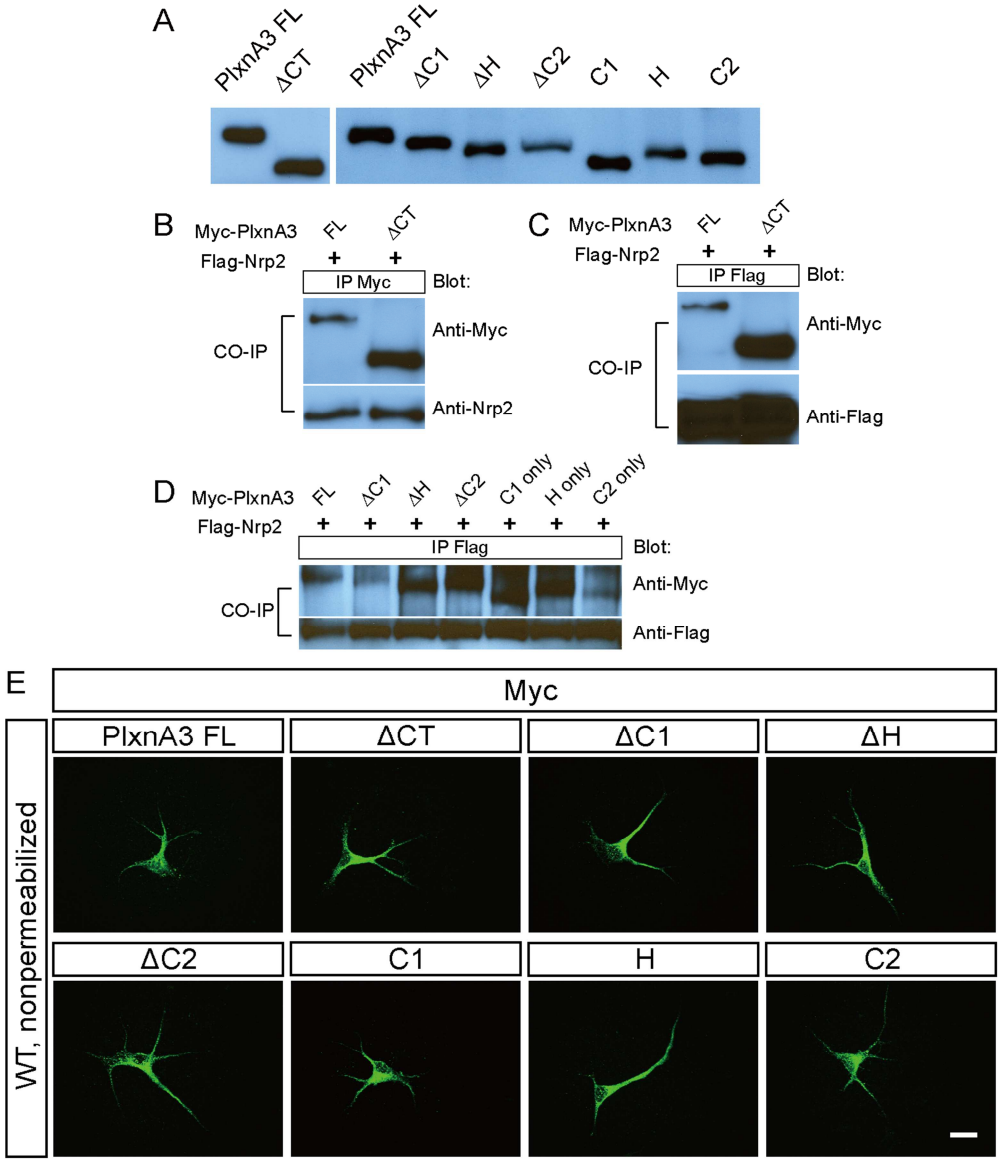

Figure 22. Validation of PlxnA3 mutants protein expression and interaction with Nrp2

(A) Western Blot of PlxnA3 mutant proteins. PlxnA3 variants were transfected into HEK293 cells for 48 hours and lysed for western blot assay using anti-Myc antibody. **(B-D)** CO-IP and western blot for PlxnA3 and Nrp2. PlxnA3 mutants and Nrp2 were co-transfected in to Hek293 cells for 48 hours and lysed for IP. (B) FL and ΔCT pull down with anti-Myc antibody. (C) FL and ΔCT pull down with anti-Flag antibody. (D) FL and rest of PlxnA3 mutants pull down with anti-Flag antibody. (E) Neuron surface expression staining. Representative images of WT E13.5 mouse cortical neurons transfected with Myc-PlxnA3 FL or PlxnA3 mutants. Neurons cultured for 6days and stained for Myc (green) with anti-Myc antibody with no Triton-X. Scale bar, 20μm.

Figure 23.

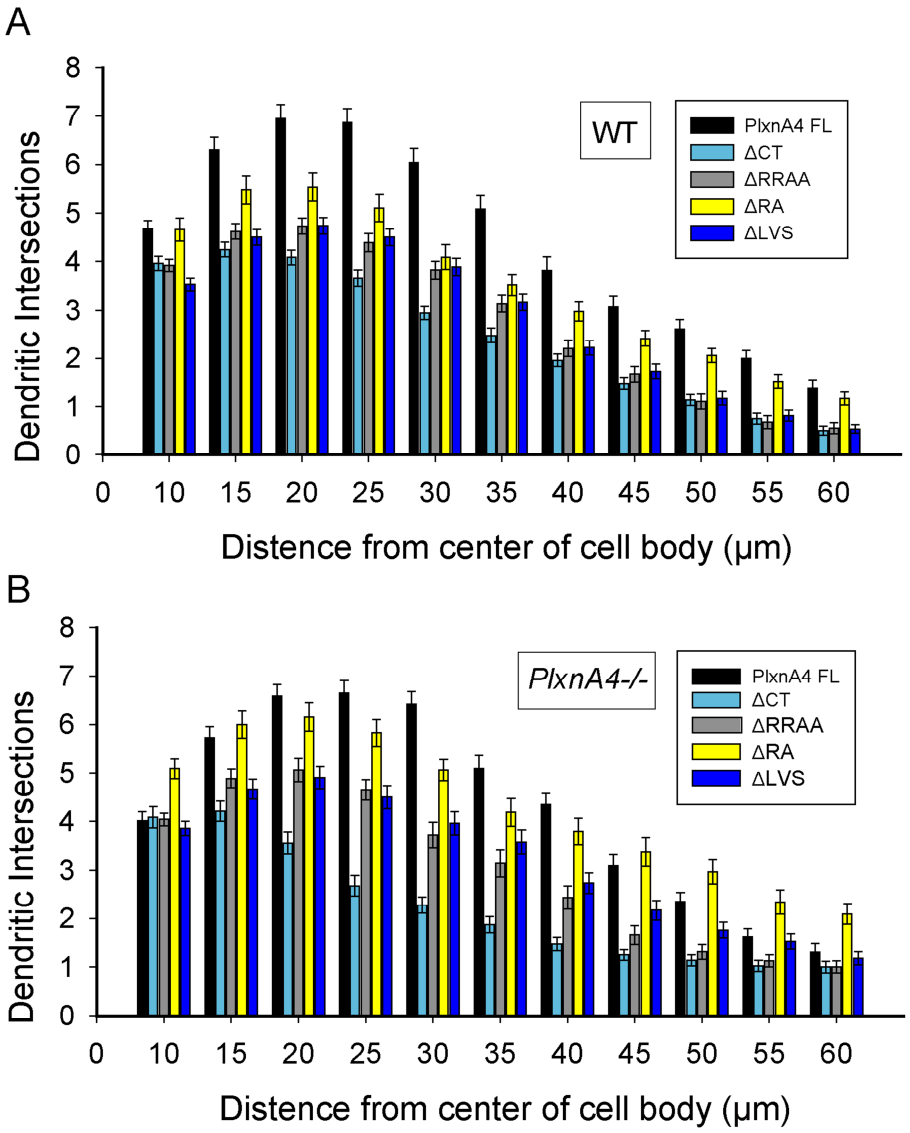

Figure 23. C1 domain LRR motif is necessary for Ras GAP activity

Dissociated cortical neurons were transfected with PlxnA4 ΔRRAA or PlxnA4 ΔRA, cultured for 6DIV and stimulate with 5nM Sema3A for 24 hours. Sholl analysis results of average dendritic intersections in (A) WT neurons (B) PlxnA4 KO neurons. N = 3 to 4 independent cultures, least 30-50 neurons were analyzed for each mutant. Data are means ± SEM.

Table 1. Plexin-A4 Constructs

Extracellular ← Intracellular →	
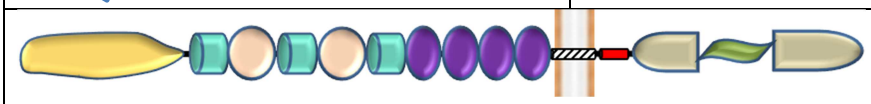	Full Length
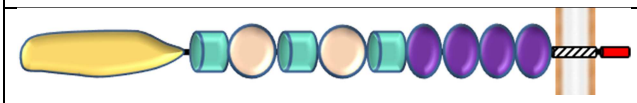	ΔCT
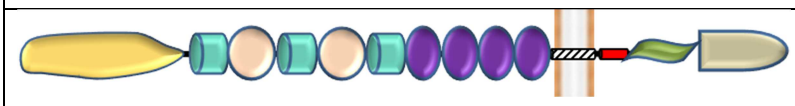	ΔC1
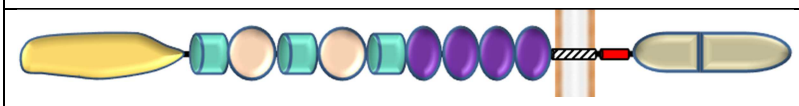	ΔH/RBD
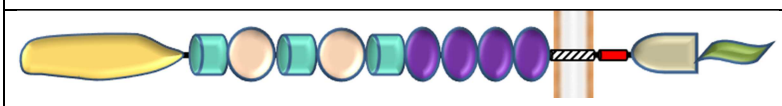	ΔC2
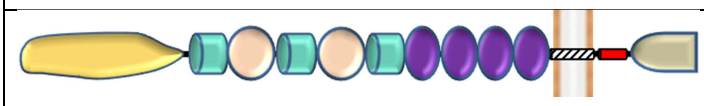	C1 only
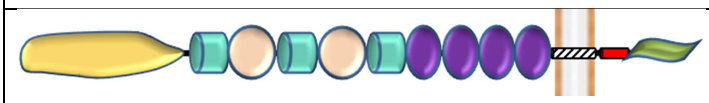	H/RBD only
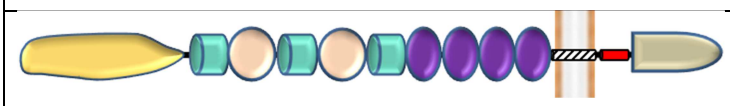	C2 only
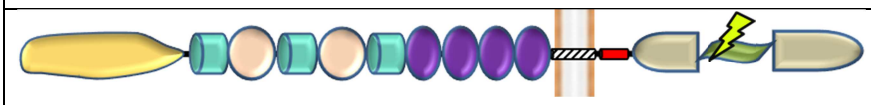	ΔLVS
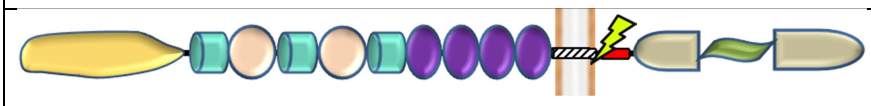	ΔKRK

Table 1. Plexin-A4 Constructs con.

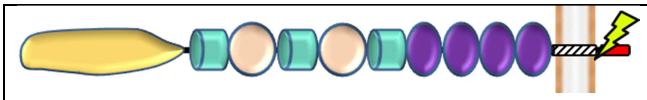	ΔCT+ΔKRK
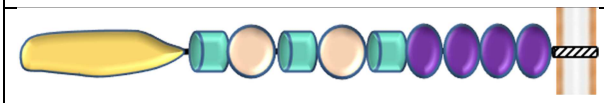	ΔCT+ΔTMC9
	ΔEcto
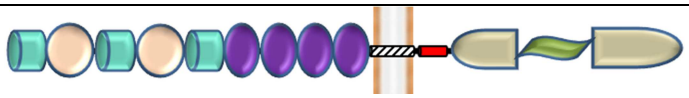	ΔSema
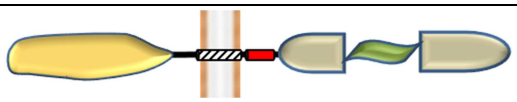	ΔIg

Table 2. Plexin-A3 Constructs

Extracellular ←	→ Intracellular	
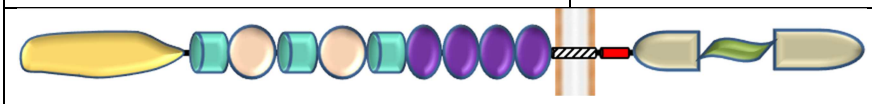		Full Length
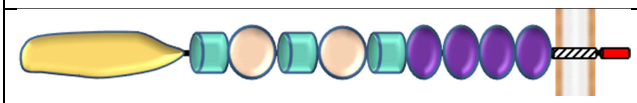		ΔCT
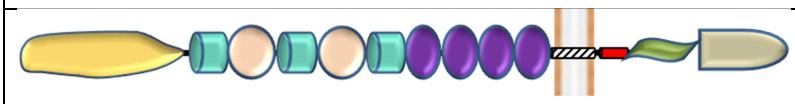		ΔC1
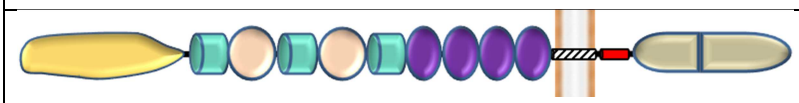		ΔH/RBD
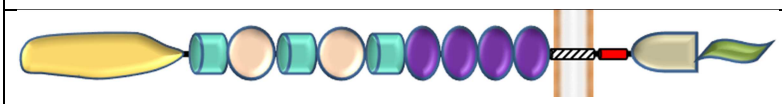		ΔC2
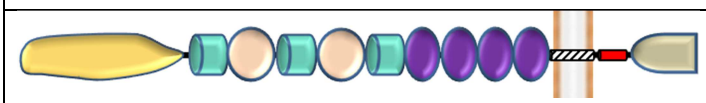		C1 only
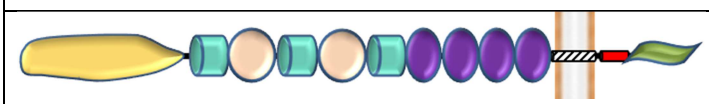		H/RBD only
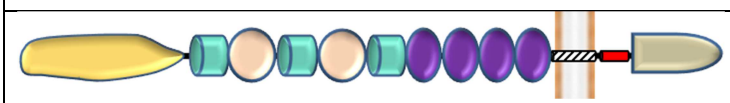		C2 only

Table 3. Primer set for Plexin-A3 cloning

Primer	Sequence	Tm(°C)
1 FWD	CCC CTCGAG GGGCTAGC AGCAGGGGGC XhoI NheI	64.5
2 REV	CCC GGCCGGCC TGGGGGGAGTATCCAGCTCCTTGA FseI	63.3
3 FWD	CCC GGCCGGCC GGTCCTATTGATGCCATAACAGGCG FseI	59.7
4 REV	CCC GGCGCGCC CTGAGACCATCTTGCTGCCGC AscI	60.9
5 FWD	CCC GGCGCGCC GAAATATATCTCACAAGGCTGCTGG AscI	55.7
6 REV	CCC GCGGCCGC GAATTC TCAGCTGCTGCTGGACA NotI EcoRI	56.9
7 REV	CCC GGCCGGCC CTTTCTCCATCTGCTGCTTGATGGCGC FesI	63.7
8 FWD	CCC GGCCGGCC TCAGAAATATATCTCACAAGGCTGCT FseI	55.9
9 REV	CCC GCGGCCGC GAATTC TGAGACCATCTTGCTGCCGC NotI EcoRI	60.4
10REV	CCC GCGGCCGC GAATTC TTTCTCCATCTGCTGCTTGATGGCGC NotI EcoRI	63.5
11REV	CCC GCGGCCGC GAATTC TCA GGGAGTATCCAGCTCCTTGA NotI EcoRI	59.1
pCAG-CFWD	AGAGCCTCTGCTAACCATGTT	56.1
PlxnA3 REV	CACCTGCTTCTCACTCAGGA	56.5

References

1. V. Fenstermaker, Y. Chen, A. Ghosh, R. Yuste, Regulation of dendritic length and branching by semaphorin 3A., *J. Neurobiol.* **58**, 403–12 (2004).

2. T. S. Tran *et al.*, Secreted semaphorins control spine distribution and morphogenesis in the postnatal CNS., *Nature* **462**, 1065–9 (2009).

3. T. Takahashi, S. M. Strittmatter, PlexinA1 Autoinhibition by the Plexin Sema Domain, *Neuron* **29**, 429–439 (2001).

4. A. Antipenko *et al.*, Structure of the semaphorin-3A receptor binding module., *Neuron* **39**, 589–98 (2003).

5. L. Ramon y Cayal, S. Swanson, Neely. Swanson, *Histology of the Nervous System of Human and Vertebrate.* (1995).

6. D. J. Solecki, E.-E. Govek, T. Tomoda, M. E. Hatten, Neuronal polarity in CNS development., *Genes Dev.* **20**, 2639–47 (2006).

7. F. C. de Anda *et al.*, Autism spectrum disorder susceptibility gene TAOK2 affects basal dendrite formation in the neocortex., *Nat. Neurosci.* **15**, 1022–31 (2012).

8. M. B. Ramocki, H. Y. Zoghbi, Failure of neuronal homeostasis results in common neuropsychiatric phenotypes., *Nature* **455**, 912–8 (2008).

9. A. L. Kolodkin, M. Tessier-Lavigne, Mechanisms and molecules of neuronal wiring: a primer., *Cold Spring Harb. Perspect. Biol.* **3** (2011), doi:10.1101/cshperspect.a001727.

10. A. B. Huber, A. L. Kolodkin, D. D. Ginty, J.-F. Cloutier, Signaling at the growth cone: ligand-receptor complexes and the control of axon growth and guidance., *Annu. Rev. Neurosci.* **26**, 509–63 (2003).

11. T. Toyofuku *et al.*, FARP2 triggers signals for Sema3A-mediated axonal repulsion., *Nat. Neurosci.* **8**, 1712–9 (2005).

12. F. Suto *et al.*, Plexin-a4 mediates axon-repulsive activities of both secreted and transmembrane semaphorins and plays roles in nerve fiber guidance., *J. Neurosci.* **25**, 3628–37 (2005).

13. F. Charron, E. Stein, J. Jeong, A. P. McMahon, M. Tessier-Lavigne, The morphogen sonic hedgehog is an axonal chemoattractant that collaborates with netrin-1 in midline axon guidance., *Cell* **113**, 11–23 (2003).

14. A. Bagri, H.-J. Cheng, A. Yaron, S. J. Pleasure, M. Tessier-Lavigne, Stereotyped pruning of long hippocampal axon branches triggered by retraction inducers of the semaphorin family., *Cell* **113**, 285–99 (2003).

15. V. Castellani, a Chédotal, M. Schachner, C. Faivre-Sarrailh, G. Rougon, Analysis of the L1-deficient mouse phenotype reveals cross-talk between Sema3A and L1 signaling pathways in axonal guidance., *Neuron* **27**, 237–49 (2000).

16. S. Chauvet *et al.*, Gating of Sema3E/PlexinD1 signaling by neuropilin-1 switches axonal repulsion to attraction during brain development., *Neuron* **56**, 807–22 (2007).

17. L. Ma, M. Tessier-Lavigne, Dual branch-promoting and branch-repelling actions of Slit/Robo signaling on peripheral and central branches of developing sensory axons., *J. Neurosci.* **27**, 6843–51 (2007).

18. P. García-López, V. García-Marín, M. Freire, Three-dimensional reconstruction and quantitative study of a pyramidal cell of a Cajal histological preparation., *J. Neurosci.* **26**, 11249–52 (2006).

19. G. N. Elston, Cortex, Cognition and the Cell: New Insights into the Pyramidal Neuron and Prefrontal Function, *Cereb. Cortex* **13**, 1124–1138 (2003).

20. R. Nieuwenhuys, The neocortex. An overview of its evolutionary development, structural organization and synaptology, *Anat. Embryol. (Berl).* **190**, 307–337 (1994).

21. N. Spruston, Pyramidal neurons: dendritic structure and synaptic integration., *Nat. Rev. Neurosci.* **9**, 206–21 (2008).

22. T. Tada, M. Sheng, Molecular mechanisms of dendritic spine morphogenesis., *Curr. Opin. Neurobiol.* **16**, 95–101 (2006).

23. T. Bonhoeffer, R. Yuste, Spine motility. Phenomenology, mechanisms, and function., *Neuron* **35**, 1019–27 (2002).

24. N. Arimura, K. Kaibuchi, Neuronal polarity: from extracellular signals to intracellular mechanisms., *Nat. Rev. Neurosci.* **8**, 194–205 (2007).

25. S. Kim, A. Chiba, Dendritic guidance., *Trends Neurosci.* **27**, 194–202 (2004).

26. E. W. Dent, F. B. Gertler, Cytoskeletal dynamics and transport in growth cone motility and axon guidance., *Neuron* **40**, 209–27 (2003).

27. K. L. Whitford *et al.*, Regulation of cortical dendrite development by Slit-Robo interactions., *Neuron* **33**, 47–61 (2002).

28. D. Bourikas *et al.*, Sonic hedgehog guides commissural axons along the longitudinal axis of the spinal cord., *Nat. Neurosci.* **8**, 297–304 (2005).

29. F. Polleux, T. Morrow, a Ghosh, Semaphorin 3A is a chemoattractant for cortical apical dendrites., *Nature* **404**, 567–73 (2000).

30. T. S. Tran, A. L. Kolodkin, R. Bharadwaj, Semaphorin regulation of cellular morphology., *Annu. Rev. Cell Dev. Biol.* **23**, 263–92 (2007).

31. A. L. Kolodkin *et al.*, Fasciclin IV: Sequence, expression, and function during growth cone guidance in the grasshopper embryo, *Neuron* **9**, 831–845 (1992).

32. Y. Luo, D. Raible, J. A. Raper, Collapsin: A protein in brain that induces the collapse and paralysis of neuronal growth cones, *Cell* **75**, 217–227 (1993).

33. A. Sakurai, C. L. Doçi, C. Doci, J. S. Gutkind, Semaphorin signaling in angiogenesis, lymphangiogenesis and cancer., *Cell Res.* **22**, 23–32 (2012).

34. U. Yazdani, J. R. Terman, The semaphorins., *Genome Biol.* **7**, 211 (2006).

35. H. Takamatsu, A. Kumanogoh, Diverse roles for semaphorin-plexin signaling in the immune system., *Trends Immunol.* **33**, 127–35 (2012).

36. R. J. Pasterkamp, Getting neural circuits into shape with semaphorins., *Nat. Rev. Neurosci.* **13**, 605–18 (2012).

37. L. Tamagnone, Emerging role of semaphorins as major regulatory signals and potential therapeutic targets in cancer., *Cancer Cell* **22**, 145–52 (2012).

38. Y. Yoshida, Semaphorin signaling in vertebrate neural circuit assembly., *Front. Mol. Neurosci.* **5**, 71 (2012).

39. R. P. Kruger, J. Aurandt, K.-L. Guan, Semaphorins command cells to move., *Nat. Rev. Mol. Cell Biol.* **6**, 789–800 (2005).

40. Y. Zhou, R.-A. F. Gunput, R. J. Pasterkamp, Semaphorin signaling: progress made and promises ahead., *Trends Biochem. Sci.* **33**, 161–70 (2008).

41. T. Takahashi *et al.*, Plexin-neuropilin-1 complexes form functional semaphorin-3A receptors., *Cell* **99**, 59–69 (1999).

42. C. Pellet-Many, P. Frankel, H. Jia, I. Zachary, Neuropilins: structure, function and role in disease., *Biochem. J.* **411**, 211–26 (2008).

43. B. J. C. Janssen *et al.*, Neuropilins lock secreted semaphorins onto plexins in a ternary signaling complex., *Nat. Struct. Mol. Biol.* **19**, 1293–9 (2012).

44. A. Yaron, P.-H. Huang, H.-J. Cheng, M. Tessier-Lavigne, Differential requirement for Plexin-A3 and -A4 in mediating responses of sensory and sympathetic neurons to distinct class 3 Semaphorins., *Neuron* **45**, 513–23 (2005).

45. B. Zhuang, Y. S. Su, S. Sockanathan, FARP1 promotes the dendritic growth of spinal motor neuron subtypes through transmembrane Semaphorin6A and PlexinA4 signaling., *Neuron* **61**, 359–72 (2009).

46. L. Menon, M.-R. Mihailescu, Interactions of the G quartet forming semaphorin 3F RNA with the RGG box domain of the fragile X protein family., *Nucleic Acids Res.* **35**, 5379–92 (2007).

47. B. Lom, S. Cohen-Cory, Brain-derived neurotrophic factor differentially regulates retinal ganglion cell dendritic and axonal arborization in vivo., *J. Neurosci.* **19**, 9928–38 (1999).

48. E. W. Dent, A. M. Barnes, F. Tang, K. Kalil, Netrin-1 and Semaphorin 3A Promote or Inhibit Cortical Axon Branching , Respectively , by Reorganization of the Cytoskeleton, *J. Neurosci.* **24**, 3002–3012 (2004).

49. L. J. Turner, S. Nicholls, A. Hall, The activity of the plexin-A1 receptor is regulated by Rac., *J. Biol. Chem.* **279**, 33199–205 (2004).

50. S. M. Zanata, I. Hovatta, B. Rohm, A. W. Püschel, Antagonistic effects of Rnd1 and RhoD GTPases regulate receptor activity in Semaphorin 3A-induced cytoskeletal collapse., *J. Neurosci.* **22**, 471–7 (2002).

51. Z. Jin, S. M. Strittmatter, Rac1 mediates collapsin-1-induced growth cone collapse., *J. Neurosci.* **17**, 6256–63 (1997).

52. K. Hong *et al.*, A ligand-gated association between cytoplasmic domains of UNC5 and DCC family receptors converts netrin-induced growth cone attraction to repulsion., *Cell* **97**, 927–41 (1999).

53. A. M. Schmitt *et al.*, Wnt-Ryk signalling mediates medial-lateral retinotectal topographic mapping., *Nature* **439**, 31–7 (2006).

54. Y. Liu *et al.*, Ryk-mediated Wnt repulsion regulates posterior-directed growth of corticospinal tract., *Nat. Neurosci.* **8**, 1151–9 (2005).

55. A. I. Lyuksyutova *et al.*, Anterior-posterior guidance of commissural axons by Wnt-frizzled signaling., *Science* **302**, 1984–8 (2003).

56. A. Sahay, M. E. Molliver, D. D. Ginty, A. L. Kolodkin, Semaphorin 3F is critical for development of limbic system circuitry and is required in neurons for selective CNS axon guidance events., *J. Neurosci.* **23**, 6671–80 (2003).

57. G. Mlechkovich *et al.*, Distinct Cytoplasmic Domains in Plexin-A4 Mediate Diverse Responses to Semaphorin 3A in Developing Mammalian Neurons, *Sci. Signal.* **7**, ra24–ra24 (2014).

58. I. Oinuma, H. Katoh, M. Negishi, Molecular dissection of the semaphorin 4D receptor plexin-B1-stimulated R-Ras GTPase-activating protein activity and neurite remodeling in hippocampal neurons., *J. Neurosci.* **24**, 11473–80 (2004).

59. M. M. Riccomagno *et al.*, The RacGAP β2-Chimaerin selectively mediates axonal pruning in the hippocampus., *Cell* **149**, 1594–606 (2012).

60. I. Oinuma, Y. Ishikawa, H. Katoh, M. Negishi, The Semaphorin 4D receptor Plexin-B1 is a GTPase activating protein for R-Ras., *Science* **305**, 862–5 (2004).

61. K. Uesugi, I. Oinuma, H. Katoh, M. Negishi, Different requirement for Rnd GTPases of R-Ras GAP activity of Plexin-C1 and Plexin-D1., *J. Biol. Chem.* **284**, 6743–51 (2009).

62. L. Cheadle, T. Biederer, The novel synaptogenic protein Farp1 links postsynaptic cytoskeletal dynamics and transsynaptic organization., *J. Cell Biol.* **199**, 985–1001 (2012).

63. H. Fujisawa, Discovery of semaphorin receptors, neuropilin and plexin, and their functions in neural development., *J. Neurobiol.* **59**, 24–33 (2004).

64. H. J. Cheng *et al.*, Plexin-A3 mediates semaphorin signaling and regulates the development of hippocampal axonal projections., *Neuron* **32**, 249–63 (2001).

65. E. a Nimchinsky, a M. Oberlander, K. Svoboda, Abnormal development of dendritic spines in FMR1 knock-out mice., *J. Neurosci.* **21**, 5139–46 (2001).

66. C. Bagni, W. T. Greenough, From mRNP trafficking to spine dysmorphogenesis: the roots of fragile X syndrome., *Nat. Rev. Neurosci.* **6**, 376–87 (2005).

Curriculum Vitae

Sheng-Shiang (Anson) Peng

Date of Birth: April 16, 1984

Birth place: Taipei, Taiwan

Address: 46 Marrow Street, Newark, NJ, USA 07103

Phone: 406-595-7323

Email: Anson.ssp@gmail.com

Education:

2014 **M.S.** Rutgers University, Department of Biological Science, Newark, NJ 07103
Major: Cell Biology and Neurobiology

2008 **M.S.** National Taiwan University, Department of Agricultural Chemistry, Taipei, Taiwan

2006 **B.S.** National Taiwan University, Department of Agricultural Chemistry, Taipei, Taiwan

Research:

Publication:

Peng, SS, Tran TS. (2014). Regulation of cortical dendrite morphology and spine organization by secreted semaphorins – A primary culture approach. JR Terman, Editor. *Humana Press, Springer Publishing Group, USA*. (*in press*)

Mlechkovich, G., **Peng, SS.**, Shacham, V., Martinez, E., Gokhman, I., Minis, A., Tran, T. S., Yaron, A. (2014). Distinct Cytoplasmic Domains in Plexin-A4 Mediate Diverse Responses to Semaphorin 3A in Developing Mammalian Neurons. (Sci. Signal., 2014 Mar; 316 (7): ra24.)

Hsieh, FC., Chen, CT., Weng, YT., **Peng, SS.,** Chen, YC., Huang, LY., Hu, HT., Wu, YL., Lin, NC., Wu, WF. (2011). Stepwise Activity of ClpY (HslU) Mutants in the Processive Degradation of Escherichia coli ClpYQ (HslUV) Protease Substrates (J Bacteriol. 2011 Oct; 193 (19): 5465-76.)

Lien, HY., Shy, RS., **Peng, SS.,** Wu, YL., Weng, YT., Chen, HH., Su, PC., Ng, WF., Chen, YC., Chang, PY., Wu, WF. (2009). Characterization of the Escherichia coli ClpY (HslU) Substrate Recognition Site of ClpYQ (HslUV) protease by the Yeast Two-Hybrid System (J Bacteriol. 2009 Jul; 191 (13):4218-31.)